



THE UNIVERSITY OF
SYDNEY

THE UNIVERSITY OF SYDNEY

AERO3261 PROPULSION

SEMESTER 1 2024

ASSIGNMENT 2

Performance of Turbofan Engines

GROUP 20

Iestyn HUGHES	530705835
Anton DEMARK	510514576
Wenjin HUANG	500045844
Thomas BULLOCK	530754154
Kyamuwendu GANYA	530706142

Executive Summary

The following report details the process of developing and analysing a hybrid-electric propulsion system for a commercial aircraft, namely the NASA STARC-ABL, intended to follow on from the Airbus A320 and Boeing 737 series. The objective was to optimise performance, whilst remaining within thermal and environmental constraints. The performance of both separate and mixed exhaust turbofan engines was investigated, as well as the degree of hybridisation, to ascertain the optimum engine for the design brief. The CFM56 engine was selected as a baseline and GASTURB was used to complete trade-off and sensitivity studies, in which design parameters were altered to observe the impact of performance. Turbine inlet temperature (TIT), fan pressure ratio (FPR) and bypass pressure ratio (BPR) were parameters that were altered in the process. Take-off was the condition in which the chosen design point was evaluated. Then, the performance in this condition was weighed against that in cruise condition. Following this, variations in performance parameters were evaluated alongside throttle setting changes, for the off-design segment. In light of the findings, a design point was selected aligning with the stipulated requirements for the cruise condition. The selected engine was a separate exhaust turbofan, with a 1.8m fan diameter and 20% DoH. In terms of design point parameters, there was an FPR of 1.65, a BPR of 7, a TIT of 1575K and a TSFC of 0.631 kg/hr/daN. The separate exhaust turbofan overall had a higher performance than the mixed configuration and the selected degree of hybridisation further enhanced performance.

Contents

Executive Summary	i
List of Figures	iv
List of Tables	v
Nomenclature	vi
1 Introduction	1
2 Engine Selection	1
2.1 Aircraft Parameters and Performance Requirements	1
2.2 Materials Research & Development	1
2.3 Production Engines	2
2.4 Constraints and Assumptions	3
2.4.1 Efficiencies	3
2.4.2 Kutta Condition	3
2.4.3 Environmental Impact	4
2.4.4 Polytropic Efficiencies	4
3 Results and Discussion	4
3.1 Parametric Study - Separate Exhaust at Design Point	4
3.1.1 FPR vs BPR	5
3.1.2 OPR vs TIT	6
3.1.3 FPR vs OPR	7
3.1.4 BPR vs TIT	8
3.1.5 Hybridisation	9
3.1.6 Installation Effects	10
3.1.7 Uniform FPR discussion	11
3.1.8 Summary of Selected Design Parameters	11
3.2 Parametric Study - Mixed Exhaust at Design Point	12
3.2.1 BPR	12
3.2.2 OPR vs TIT	13
3.2.3 FPR vs OPR	14

3.2.4	BPR vs TIT	15
3.2.5	Hybridisation	16
3.2.6	Installation Effects	18
3.2.7	Summary of Selected Design Parameters	18
3.3	Engine Architecture Comparison	19
3.4	Sensitivity Study	20
3.5	Final Design Point Selection	21
3.6	Off-Design Performance	22
4	Conclusion	25
	References	xxvi
A	Supporting Figures	xxvii
A.1	Separate Exhaust Study	xxvii
A.1.1	OPR vs TIT	xxvii
A.1.2	BPR vs TIT	xxviii
A.2	Mixed Exhaust Study	xxviii
B	Mixed Fan Pressure Ratio Notes	xxix
B.1	Figures	xxix
B.2	Discussion	xxx
C	GASTURB for Separate	xxx
C.1	Iteration Parameters	xxx
C.2	Composed Variables	xxx
C.3	Design Point Cycle	xxxii
D	GASTURB for Mixed	xxxv
D.1	Iteration Parameters	xxxv
D.2	Composed Variables	xxxv
D.3	Design Point Cycle	xxxvii
E	GASTURB for Off-design	xl
E.1	Off-Design Point Cycle	xl

List of Figures

3.1	A separate exhaust parametric plot describing the variation in installed TSFC [kg/hr/daN] and installed Specific Thrust [daN/kg/s] with Bypass Ratio (BPR) and Fan Pressure Ratio (FPR).	5
3.2	A separate exhaust parametric plot describing the variation in installed TSFC [kg/hr/daN] and installed Specific Thrust [daN/kg/s] with Overall Pressure Ratio (OPR) and Turbine Inlet Temperature (TIT).	6
3.3	A separate exhaust parametric plot describing the variation in installed TSFC [kg/hr/daN] and installed Specific Thrust [daN/kg/s] with Overall Pressure Ratio (OPR) and Fan Pressure Ratio (FPR).	7
3.4	A separate exhaust parametric plot describing the variation in installed TSFC [kg/hr/daN] and installed Specific Thrust [daN/kg/s] with Bypass Ratio (BPR) and Turbine Inlet Temperature (TIT). This was plotted from the side wherein F_{spec} was aligned into the page.	8
3.5	A separate exhaust parametric plot describing the variation in installed TSFC [kg/hr/daN] and installed Specific Thrust [daN/kg/s] with HPCPR and TIT. This was repeated for three fixed-degrees of Hybridisation (DoHs).	9
3.6	A separate exhaust parametric plot comparing the variation in TSFC [kg/hr/daN] and Specific Thrust [daN/kg/s] with HPCPR and TIT for uninstalled and installed performance.	10
3.7	A separate exhaust parametric plot comparing the variation in TSFC [kg/hr/daN] and Specific Thrust [daN/kg/s] with HPCPR and TIT for three different radial pressure distributions.	11
3.8	A mixed exhaust parametric plot describing the variation in installed TSFC [kg/hr/daN] and installed Specific Thrust [daN/kg/s] with BPR	12
3.9	A mixed exhaust parametric plot describing the variation in installed TSFC [kg/hr/daN] and installed Specific Thrust [daN/kg/s] with Overall Pressure Ratio (OPR) and Turbine Inlet Temperature (TIT).	13
3.10	A mixed exhaust parametric plot describing the variation in installed TSFC [kg/hr/daN] and installed Specific Thrust [daN/kg/s] with Bypass Ratio (BPR) and Overall Pressure Ratio (OPR)	15
3.11	A mixed exhaust parametric plot describing the variation in installed TSFC [kg/hr/daN] and installed Specific Thrust [daN/kg/s] with Bypass Ratio (BPR) and Turbine Inlet Temperature (TIT). This was plotted from the side wherein F_{spec} was aligned into the page.	16
3.12	A mixed exhaust parametric plot describing the variation in installed TSFC [kg/hr/daN] and installed Specific Thrust [daN/kg/s] with HPCPR and TIT. This was repeated for three fixed-degrees of Hybridisation (DoHs).	17
3.13	A mixed exhaust parametric plot comparing the variation in TSFC [kg/hr/daN] and Specific Thrust [daN/kg/s] with HPCPR and TIT for uninstalled and installed performance.	18

3.14	The variation in operating line of the HPC at takeoff and cruise	22
3.15	The variation in operating line of the LPC at takeoff and cruise	22
3.16	The variation in operating line of the booster at takeoff and cruise	23
3.17	The variance in BPR and TSFC with throttle setting.	24
3.18	The variance in LPR, OPR and specific thrust with throttle settings.	25
A.1	A separate exhaust parametric plot describing the variation in installed TSFC [kg/hr/daN] and installed Specific Thrust [daN/kg/s] with Overall Pressure Ratio (OPR) and Turbine Inlet Temperature (TIT). This was plotted from the side wherein F_{spec} was aligned into the page.	xxvii
A.2	A separate exhaust parametric plot describing the variation in installed TSFC [kg/hr/daN] and installed Specific Thrust [daN/kg/s] with Bypass Ratio (BPR) and Turbine Inlet Temperature (TIT) in a standard view.	xxviii
A.3	A mixed exhaust parametric plot describing the variation in installed TSFC [kg/hr/daN] and installed Specific Thrust [daN/kg/s] with Bypass Ratio (BPR) and Turbine Inlet Temperature (TIT) in standard view.	xxviii
B.1	A mixed exhaust parametric plot describing the variation in installed TSFC [kg/hr/daN] and Fan Pressure Ratio with Overall Pressure Ratio (OPR)	xxix
B.2	A mixed exhaust parametric plot describing the variation in installed TSFC [kg/hr/daN] and Fan Pressure Ratio with Turbine Inlet Temperature (TIT) [K]	xxix
C.1	Iteration variables in for separate exhaust GASTURB window.	xxx
D.1	Iteration variables in for mixed exhaust GASTURB window.	xxxv

List of Tables

0.1	Nomenclature and Units	vi
2.1	STARC-ABL parameters (metric units).	1
2.2	STARC-ABL Performance Requirements (metric units).	1
2.3	Engine Specifications [4]	2
3.1	Selected design point parameters for the separate-exhaust configuration.	12
3.2	Selected design point parameters for the mixed-exhaust configuration.	19
3.3	Sensitivity study conducted at the selected design point for separate and mixed exhaust engines at cruise	20
3.4	Selected design point parameters for the final configuration.	21

Nomenclature

For concision, shorthand acronyms and symbols were used throughout this report as recorded in Table 0.1.

Table 0.1: Nomenclature and Units

Symbol	Description	Units
A	Area	m ²
BCF	Blade Cooling Fraction	-
BLI	Boundary Layer Ingestion	-
BPR	Bypass ratio	-
d_{fan}	Fan Diameter	m
DoH	Degree of Hybridisation	-
F	Thrust	N
$F_{N,I}$	Net Thrust Installed	N
F_N	Net Thrust	N
F_{spec}	Specific Thrust	N/kg
$FAR \left(\frac{\dot{m}_{fuel}}{\dot{m}_{air}} \right)$	Fuel-to-Air Ratio	-
FPR or π_{fan}	Fan Pressure Ratio	-
HPCPR or π_{HPC}	High Pressure Compressor Ratio	-
HPT	High Pressure Turbine	-
IFPR or $\pi_{fan,inner}$	Inner Fan Pressure Ratio	-
IPC	Intermediate Pressure Compressor	-
IPCPR or π_{IPC}	Intermediate Pressure Compressor Pressure Ratio	-
LPT	Low Pressure Turbine	-
\dot{m}_p	Primary Mass Flow Rate	kg/s
\dot{m}_s	Secondary Mass Flow Rate	kg/s
NO _x	Nitrogen Oxides	-
OFPR or $\pi_{fan,outer}$	Outer Fan Pressure Ratio	-
OPR or $\pi_{overall}$	Overall Pressure Ratio	-
P	Power	W
p	Pressure	Pa
RCF	Rotor Cooling Fraction	-
ST or F_{spec}	Specific Thrust	daN/kg/s
T	Temperature	K
TIT or T_4	Turbine Inlet Temperature	K
TSFC	Thrust Specific Fuel Consumption	kg/hr/daN
V	Velocity	m/s
W_{engine}	Weight of Engine	N
η_{core}	Core Efficiency	-
η_{prop}	Propulsive Efficiency	-
η_p	Polytropic Efficiency	-
γ	Specific Heat Ratio	-

1 Introduction

The project was centred on determining the optimal engine design for a hybrid passenger aircraft, in service of an aeronautical consultancy company. A research contract had been attained from a venture capital fund, and UsydAir was funded in pursuing this development. Using GasTurb software, an analysis of turbofan engine configurations was conducted and comparisons drawn. Starting from the baseline of the CFM56 engine, as per design specifications, analysis was carried out at off-design conditions at the top-of-climb. Trade-off studies were also completed and off-design performance was assessed on advanced designs to identify the engine solution most efficient for use. These studies were undertaken for both separate and mixed turbofans at design point across a range of design parameters; alongside sensitivity studies focused on the impact of design parameters on engine performance.

2 Engine Selection

2.1 Aircraft Parameters and Performance Requirements

The study was completed for NASA's proposed STARC-ABL aircraft [1], for which the critical parameters were given in Table 2.1 and the performance requirements were given in Table 2.2.

Table 2.1: STARC-ABL parameters (metric units).

Number of Engines	2	Cruise Mach Nr	0.8
Date of First Flight	2035	Nr of Passengers	180
Max Gross TO Weight [N]	60,160	Wing Aspect Ratio [-]	8.3
Operational Empty Weight [N]	34,155	Flight Ceiling [m]	13,716
Max Fuel Capacity [N]	8,777		

Table 2.2: STARC-ABL Performance Requirements (metric units).

	Uninstalled Thrust [N]	Mach Nr	Altitude [m]
Take-Off	126,063	0.20	0
Top-Of-Climb	30,248	0.80	10,668

2.2 Materials Research & Development

Material selection is dependant on the intrinsic properties of individual components. For a turbofan architecture - this is centred on improving efficiency and performance. Polymeric composites are used for the inlet and fan primarily due to the weight-saving benefits afforded by their high strength-to-weight ratios. However, this only applies in the lower reaches of the temperature range restricting the usage to colder components.

Titanium alloy is used at the leading edge of the fan blades to mitigate against bird-strike damage, as polymeric composites lag behind in impact resistance make them brittle by comparison [2].

For the compressor material, high-temperature strength is of emphasis; therefore steel, nickel, and titanium-based alloys are chosen. For the combustion chamber, it is ostensibly a selection based on temperature resistance, which leads to cobalt and nickel-based ‘super-alloys’. Moving aft, the turbine blades are subjected to extreme temperature conditions, leaving them vulnerable to: fatigue, creep, and corrosion. To combat these challenges, it is common to use nickel-based super-alloys.

Before nickel-based alloys became widespread, cobalt-based super-alloys were more prevalent; developing a nickel-based solution was challenging, despite the abundance of the Nickel making raw-material costs low. More specifically, the emergence of advanced single-crystal fabrication enabled the composition of the super-alloys to be precisely specified. These improved tolerances were a catalyst for greater creep and thermal fatigue resistance.

The metal temperature is assumed not to be in excess of 1250K, as stipulated within the brief, however, in actuality in the average commercial jet engine, the combustion chamber reaches in the region of 2300K, hence in actuality bespoke cooling methods are required to maintain operation [3].

2.3 Production Engines

Table 2.3: Engine Specifications [4]

Parameter	RCo.12 Mk.509A	IAE V2500-A1	CFM56- 7B24	PW6124	CFM LEAP-1A
BPR [-]	0.3	5.4	5.3	4.8	11
Compressor Stages [-]	1, 7, 9	1, 3, 10	1, 3, 9	1, 4, 5	1, 3, 10
Dry Weight [kg]	2061	2404	2366	2449	3150
FPR [-]	1.5	1.65	-	-	-
Net Thrust [kN]	78	110	108	106	97
OPR [-]	14.1	29.4	26	29.6	50
Year [-]	1956	1989	1997	2006	2013

The following ranges were selected for the associated parameters:

- FPR: 1.3 to 1.8
- BPR: 4 to 11

- HPCPR: 8.5 to 12.5
- TIT: 1300K to 1750K

These values were selected based on the data displayed above in Table 2.3. There was a limited set of data available for FPR, so the range was chosen to be larger to ensure a useful set of results. BPR was chosen on the range present, excluding the low bypass ratio Rolls-Royce engine. The OPR range was chosen in a similar manner. However, OPR was made up of the pressure ratios of the individual components. The fan pressure ratios were fixed by their matching and the Kutta condition, so the high pressure compressor (HPC) pressure ratio was used to vary OPR in **GASTURB**. Literature data for the turbine inlet temperature was not able to be obtained, so the limits were defined based on the design criteria. In general, the trend of BPR, FPR and OPR indicated that as the engines become more modern, these ratios increased. As such, the range selected utilised the upper end of the data present to reflect the technological trend. The 1956 Rolls-Royce engine parameters were neglected as modern engine design has far outstripped the technology used in the Rolls-Royce. The Rolls-Royce engine was included the research to provide a baseline example from which design has evolved from. Note that the ranges described above were used as guidelines - some variation was made during the **GASTURB** iteration to increase plot readability.

2.4 Constraints and Assumptions

2.4.1 Efficiencies

In terms of thermal restrictions, the maximum turbine inlet temperature was stipulated, to ensure operation safely within material limits. At take-off and initial climb, the turbine inlet temperature was limited to 1900K, whilst in top-of-climb condition, the temperature could not be greater than 1750K. Similarly, the compressor discharge temperature was limited to 900K, as this controls the thermal strain on the compressor and components further downstream. Limiting the turbine inlet temperatures also pertained to cooling, especially for the high pressure turbine. Seeing as, cooling air originates from the compressor discharge, meaning a greater need for cooling diminishes the turbine efficiency. The diameter of the fan was restricted to 1.8m, because the STARC-ABL is a commercial aircraft designed to replace the Boeing 737-800 and Airbus A320. Meaning, the aircraft must have a similar fan diameter to its predecessors. Further to this, the fan diameter has a considerable impact on the total weight and drag of the engine, therefore increasing this parameter adversely affects fuel consumption and efficiency. The nozzle was assumed to be adiabatic as well, meaning that there is no consideration for the heat transfer of air within the nozzle.

2.4.2 Kutta Condition

The Kutta condition stipulates that the bypass air rejoining and the core flow of air must be of equal pressure. The mixed exhaust engine has the Kutta condition, wherein $p_{t25} = p_{t5}$, whilst the separate engine did not have this constraint. This is because the bypass flow does not rejoin the core flow prior to exiting the engine. Therefore, an

additional iteration was necessary to accommodate this condition $p_{t25} = p_{t5}$, using the OFPR. The Kutta condition yields a single FPR for a given OPR, BPR and TIT, thus this was a constraint that had to be considered.

2.4.3 Environmental Impact

From an environmental perspective, nitrogen oxides (NOx) emissions are a constraint, since this an area in which heavy regulation has come to pass in the aviation industry. This is the primary emission of interest, as the extremely high temperatures and pressures in combustion mean conditions are an ideal breeding ground for NOx emissions. The profound impact on air quality and the contribution to acid rain, serve as examples of why these emissions are tightly monitored in society and government. Hence, there is a trade-off between engine performance and environmental impact, as modern aircraft must be deemed sustainable.

2.4.4 Polytypic Efficiencies

The polytypic efficiency of a compressor is reduced for greater pressure ratios [5]. Therefore, a linear reduction of stage pressure ratio was considered, where the pressure ratio of each compressor was determined by $\pi_{stage} = (\pi_{compressor})^{\frac{1}{n}}$ for n stages. The resulting expressions were given in Equation 2.1.

$$\begin{aligned}\eta_{poly, fan} &= -\frac{1}{30}\pi_{stage} + \frac{24}{25} \\ \eta_{poly, IPC} &= -\frac{1}{10}\pi_{stage} + \frac{21}{20} \\ \eta_{poly, HPC} &= -\frac{2}{15}\pi_{stage} + \frac{11}{10}\end{aligned}\tag{2.1}$$

Cooling air also reduces the polytypic efficiency of a turbine. As only the HPT was cooled, the LPT polytypic efficiency was considered constant. For the HPT, the reduction in $\eta_{poly, HPT}$ was approximated as $\eta_{poly, HPT} - \frac{W_{cool}}{W}$, where $\frac{W_{cool}}{W}$ was the cooling fraction of air circumventing combustion.

3 Results and Discussion

3.1 Parametric Study - Separate Exhaust at Design Point

To explore the viability of a separate-exhaust turbofan configuration for the NASA STARC-ABL, a parametric study was completed. The study was performed for cruise conditions at the ‘top of climb’ design point (cruise altitude but with some margin for manoeuvres). The four metrics outlined in Section 2 were varied pairwise in all meaningful permutations, forming plots for FPR vs BPR, OPR vs TIT, FPR vs OPR, and BPR vs TIT. Each parametric study was plotted for TSFC and F_{spec} , with installation effects taken into account. Parameters not explicitly varied in each parametric study were

held constant at their baseline parameters: $\pi_{IPC} = 1.81$, $\pi_{fan,inner} = \pi_{fan,outer} = 1.6$. The HPC exit, LPT inlet, and fan diameter constraints justified in Section 2 were also implemented.

Throughout the study, F_N was iterated to meet the total thrust requirement for the design point. As F_N remained unchanged ($F_N = C = 15.1kN$), Equation 3.1 must remain balanced [5].

$$F_N = \dot{m}_p [(1 + FAR)V_9 - V_0] + \dot{m}_s (V_{19} - V_0) + A_9(p_9 - p_0) + A_{19}(p_{19} - p_0) \quad (3.1)$$

3.1.1 FPR vs BPR

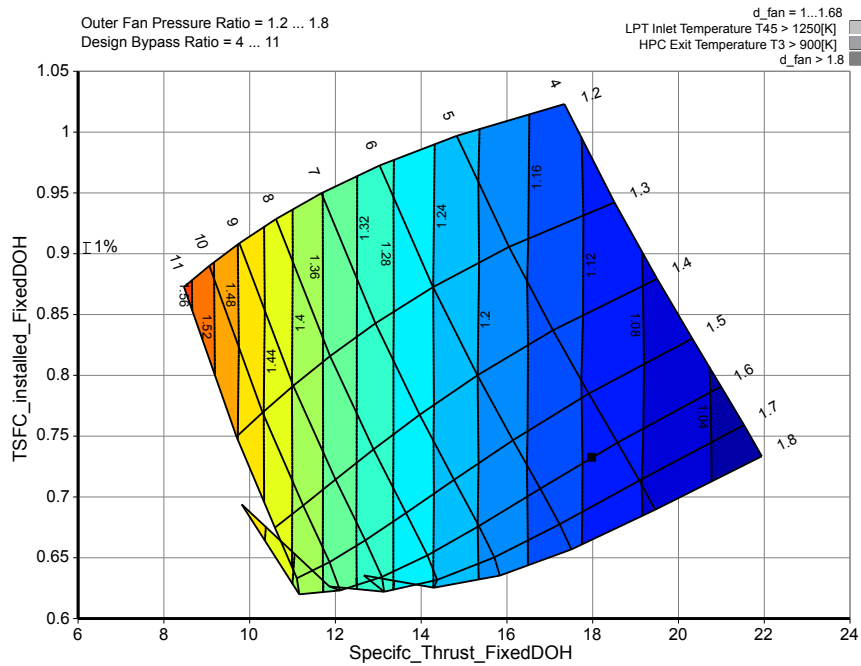


Figure 3.1: A separate exhaust parametric plot describing the variation in installed TSFC [kg/hr/daN] and installed Specific Thrust [daN/kg/s] with Bypass Ratio (BPR) and Fan Pressure Ratio (FPR).

For the first investigation, FPR was varied against BPR to produce Figure 3.1. In Figure 3.1, the installed TSFC and F_{spec} ($TSFC_I$ and $F_{spec,I}$) decreased with increasing BPR for a fixed FPR. The decrease in $TSFC_I$ with BPR was greatest along isolines of a lower FPR (towards the top of Figure 3.1), as indicated by their steeper gradient. These isolines flattened for higher values of FPR (towards the bottom), wherein increases in BPR produced smaller decreases of $TSFC_I$, and therefore smaller efficiency gains.

$F_{spec,I}$ decreased with BPR as expected, as $F_N = C$ and $F_N = F_{spec} \cdot \dot{m}_p(1 + BPR)$, F_{spec} must decrease as BPR grows. The size of reduction in F_{spec} also shrank for higher BPRs and hence larger engines, as seen by narrowing contours moving from right to left in Figure 3.1. This was explained by the $(1 + BPR)$ term, which grows rapidly w.r.t to F_{spec} for small BPRs but has a much smaller proportional impact for higher BPRs, trending asymptotically towards zero for an infinitely large engine.

For a fixed BPR, increasing FPR reduced the engine size needed as indicated by BPR-isolines of negative gradient. Increased FPR with fixed BPR also increased efficiency (lowering $TSFC_I$ and raising $F_{spec,I}$) – this was caused by FPR increasing V_{19} in Equation 3.1, such that the bypass flow developed more thrust w.r.t to the core. Therefore for constant BPR, FAR was reduced to satisfy $F_N = C$. This phenomenon led to divergent behaviour for high-FPR performance, producing discontinuities on the lower edge of Figure 3.1, where BPR could not be increased. Along high-FPR isolines (e.g FPR = 1.8), V_{19} dominates and the engine core thrust is low due to low FAR. In the limiting case, the LPT is not able to generate enough power from the core flow to drive the larger fan needed to increase BPR.

Following analysis of Figure 3.1, it was identified that FPR was the critical parameter impacting $TSFC_I$. A conservative FPR of $\approx 1.6 \rightarrow 1.7$ was selected. For BPR, a broad range of BPRs $\approx 5 \rightarrow 8$ were chosen to be refined following the BPR-TIT study outlined in Section 3.1.4.

3.1.2 OPR vs TIT

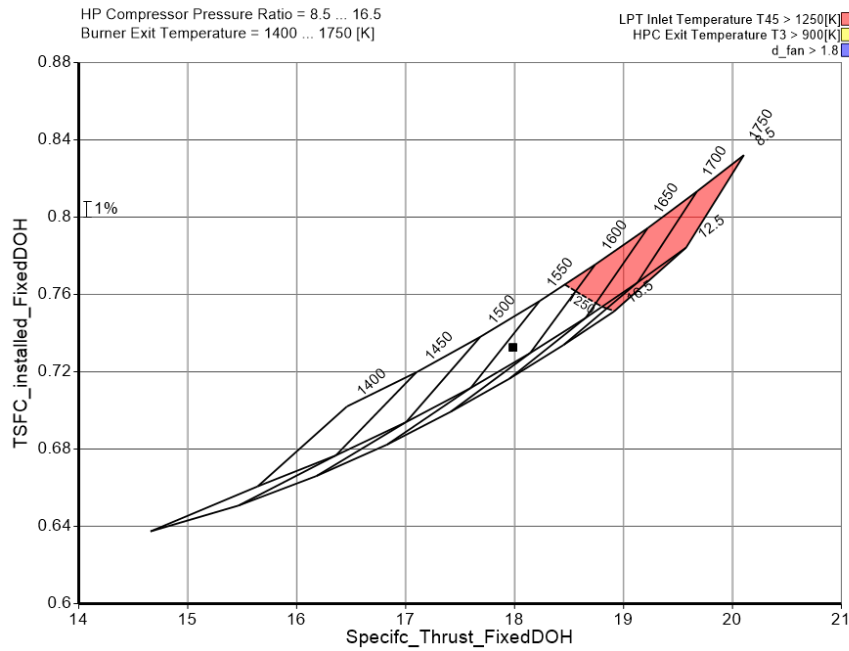


Figure 3.2: A separate exhaust parametric plot describing the variation in installed TSFC [kg/hr/daN] and installed Specific Thrust [daN/kg/s] with Overall Pressure Ratio (OPR) and Turbine Inlet Temperature (TIT).

For the second investigation, OPR was varied against TIT to produce Figure 3.2. As OPR is not available as a parameter to be varied in **GASTURB**, the range of OPR selected in Section 2 were translated to a range of HPCPC using $\pi_{HPC} = \pi_{overall} / (\pi_{fan} \cdot \pi_{booster})$.

For discussion, Figure 3.2 was plotted in a standard view with F_{spec} on the horizontal axis. The same results were also plotted in a side view where $TSFC_I$ trends may be clearer in Figure A.1 (Appendix A.1). Figure 3.2 was limited in high-TIT, low-OPR performance by the material limits of the LPT. As LPT blades were not cooled, a boundary was added

to ensure the metal temperature did not exceed the restriction identified in Section 2. The region exceeding this boundary was shaded in red.

Along an isoline of HPCPR (and hence OPR), $TSFC_I$ increased with TIT. This was explained simply – as TIT increases, \dot{m}_f is increased, burning more fuel and reducing TSFC for a fixed thrust. To satisfy $F_N = C$ whilst increasing TIT, the engine size must decrease to counteract the increased V_9 in Equation 3.1, which will in turn increase core thrust. $F_{spec,I}$ also increased with TIT; as engine size was reduced, \dot{m}_a was decreased for $F_N = C$, raising F_{spec} . Conversely, for a fixed TIT with increasing OPR, $TSFC_I$ and $F_{spec,I}$ both decrease. This trend converges towards a single isoline at $\approx HPCPR = 14$. Whilst this trend does reverse (i.e creating a concave parametric plane) for $HPCPR \gg 20$, these design points exceeded the HPC exit temperature constraint and so were not considered.

From this study, it was concluded that OPR (HPCPR) should be pushed closed to the convergent region, without being increased unnecessarily (as any $TSFC_I$ gain would be offset by the drag and weight penalties of a larger engine). Therefore, HPCPR should be $\approx 12 \rightarrow 14$. TIT was then selected as a trade-off between improved installation and F_{spec} performance (a smaller engine needed for higher TIT) and an increased TSFC for high TIT, prompting a selected range of $\approx 1550K \rightarrow 1600K$. Whilst this may seem high from Figure 3.2, this was justified in later discussion of a BPR-TIT study, and the impact of hybridisation in Sections 3.1.4 and 3.1.5.

3.1.3 FPR vs OPR

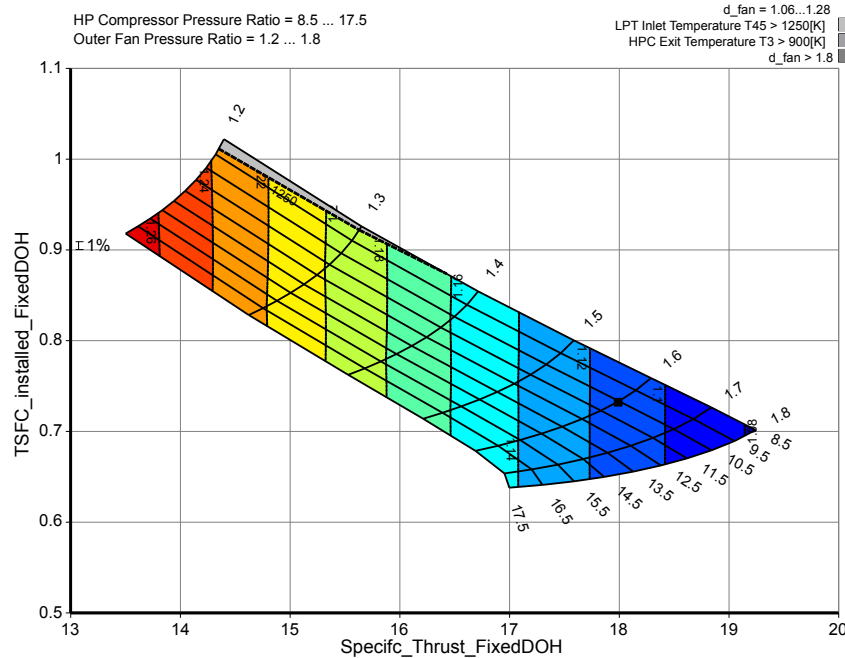


Figure 3.3: A separate exhaust parametric plot describing the variation in installed TSFC [kg/hr/daN] and installed Specific Thrust [daN/kg/s] with Overall Pressure Ratio (OPR) and Fan Pressure Ratio (FPR).

For the third investigation, FPR was varied against OPR to produce Figure 3.3. Figure 3.3 showed that for a fixed FPR, $TSFC_I$ and $F_{spec,I}$ both decreased with increasing

HPCPR (and hence OPR). As OPR is increased, T_{t3} grows, therefore the \dot{m}_f required to reach TIT is lowered, improving efficiency and reducing $TSFC_I$. The d_{fan} contour revealed that engine size decreased slightly along these FPR isolines. This was explained by Equation 3.1: as OPR is increased, a leaner FAR is needed whilst the thrust output must be maintained ($F_N = C$). As such, engine size must be increased, increasing \dot{m}_a and explaining the consequent drop in F_{spec} .

For a fixed OPR and increasing FPR, $TSFC_I$ decreased yet F_{spec} increased. This trend was observed in Figure 3.1 and discussed in detail in Section 3.1.1. The divergence seen in Figure 3.1 also produced irregularity in Figure 3.3, presenting a limitation to be carefully considered. For the flatter near-horizontal high-FPR isolines, it was noted that the TSFC penalty for a lower HPCPR (and thus improved F_{spec}) was reduced, encouraging a lower HPCPR for selection. This formed a trade-off to be balanced with the higher HPCPR favoured from Figure 3.2.

Overall, from this study it was identified that FPR was the dominant parameter governing performance in Figure 3.3. As such, it was suggested that FPR should be ≈ 1.65 , providing strong performance whilst well-away from the limit explored in Section 3.1.1. This FPR was complimented by the selected HPCPR range of $\approx 12 \rightarrow 14$ from Figure 3.2, for which a wide range of TIT's remained attainable.

3.1.4 BPR vs TIT

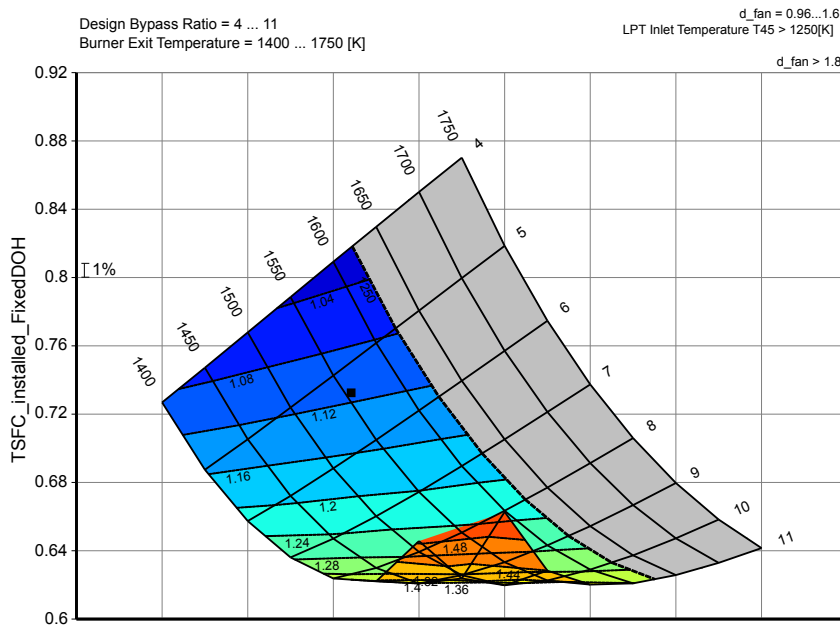


Figure 3.4: A separate exhaust parametric plot describing the variation in installed TSFC [kg/hr/daN] and installed Specific Thrust [daN/kg/s] with Bypass Ratio (BPR) and Turbine Inlet Temperature (TIT). This was plotted from the side wherein F_{spec} was aligned into the page.

For the fourth investigation, BPR was varied against TIT to produce Figure 3.4. The same results were also plotted in standard view with F_{spec} on the horizontal as shown in Figure A.2 (Appendix A.1).

In Figure 3.4, an increase in TIT for fixed-BPR resulted in an increased $TSFC_I$ with a reduced engine size as indicated by the d_{fan} contours. This was expected – a richer FAR (and thereby greater \dot{m}_f) was needed to maintain $F_N = C$ in the smaller engine (Equation 3.1).

Along a TIT-isoline of increasing BPR, the trend exhibited an inflection point. For low BPRs, $TSFC_I$ initially decreased; the core flow is reduced such that less fuel is required to reach the fixed TIT. The thrust deficit is counteracted by a larger fan, which increases the secondary thrust to maintain $F_N = C$. However at the inflection point (BPR ≈ 9) the reduced core flow is not able to produce enough power in the turbines to drive the fan. Beyond this BPR, the core flow must be increased to feed a larger fan, snowballing the engine-size requirement. This effect was most pronounced for low-TIT isolines

From this study, it was concluded that a high-BPR engine must be carefully bounded in TIT. A TIT $< 1500K$ risked needing an excessively large engine, whilst a TIT > 1620 would exceed the thermal limits (1250K) of the un-cooled LPT blades.

3.1.5 Hybridisation

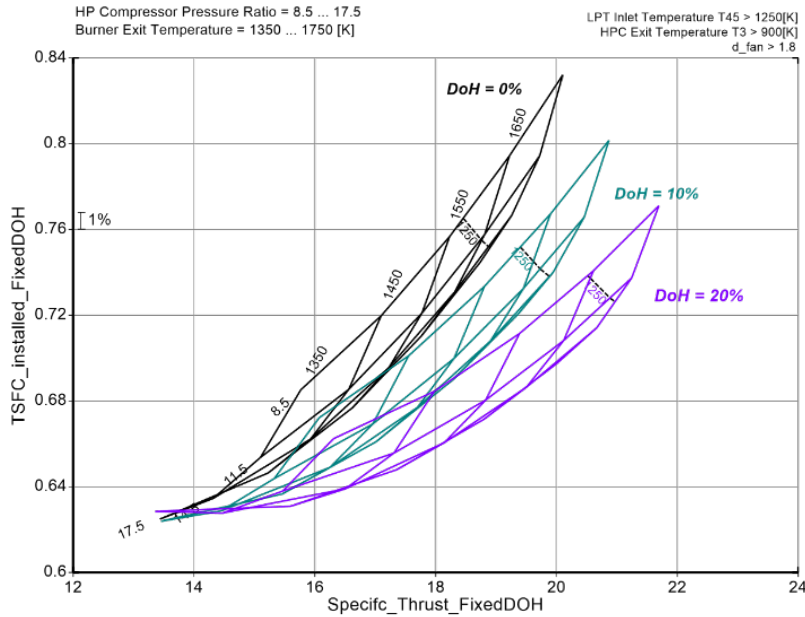


Figure 3.5: A separate exhaust parametric plot describing the variation in installed TSFC [kg/hr/daN] and installed Specific Thrust [daN/kg/s] with HPCPR and TIT. This was repeated for three fixed-degrees of Hybridisation (DoHs).

To investigate the impact of increasing the degree of hybridisation, the study to produce Figure 3.2 was repeated for three hybridisation factors (0%, 10% and 20%) and plotted as Figure 3.5. DoH $> 20\%$ failed to converge within GASTURB, presenting an upper boundary for testing. For this case, F_N was no longer considered constant. Instead, a total thrust condition was used for iteration, where $F_{TOTAL} = 2F_N + F_{BLI} = 30.2kN$. Using the total thrust condition, F_N was found to reduce with F_{BLI} , and hence DoH.

In Figure 3.5, it was observed that the design point envelope was rotated towards the horizontal, reducing $TSFC_I$ and increasing F_{spec} , significantly improving engine perfor-

mance. The boundary layer ingestion (BLI) fan was configured to draw power from the main turbofans' turbines such that $2P_{turb} = 2P_{comp} + P_{BLI}$.

To explain the behaviour observed in Figure 3.5, a fixed engine configuration was considered (constant FPR, OPR, BPR, TIT, γ and η), although the engine size itself was not constrained. For an increased DoH, more energy is bled from the engines to be supplied to the BLI fan, reducing V_9 and therefore F_N to maintain the total thrust criterion. Therefore, less power is supplied to the main-engine fan, requiring a small fan diameter (reducing \dot{m}) and reducing the fuel flow (\dot{m}_f) needed to achieve TIT. Therefore, for a constant F_{TOTAL} (per engine) = 15.1kN, $TSFC$ was reduced whilst F_{spec} was increased.

For a separate exhaust architecture, F_{BLI} is not strongly coupled to F_{bypass} – which produces the majority of the engine thrust. This independence allows hybridisation to be favourable for a separate exhaust design. The upper bound on DoH was then described clearly as the point at which the reduced flow rate through the core is not sufficient to drive air through the engine, preventing GASTURB from converging. Overall, it was concluded that the maximum feasible degree of hybridisation should be used for the separate engine. Therefore, DoH was selected = 20%.

3.1.6 Installation Effects

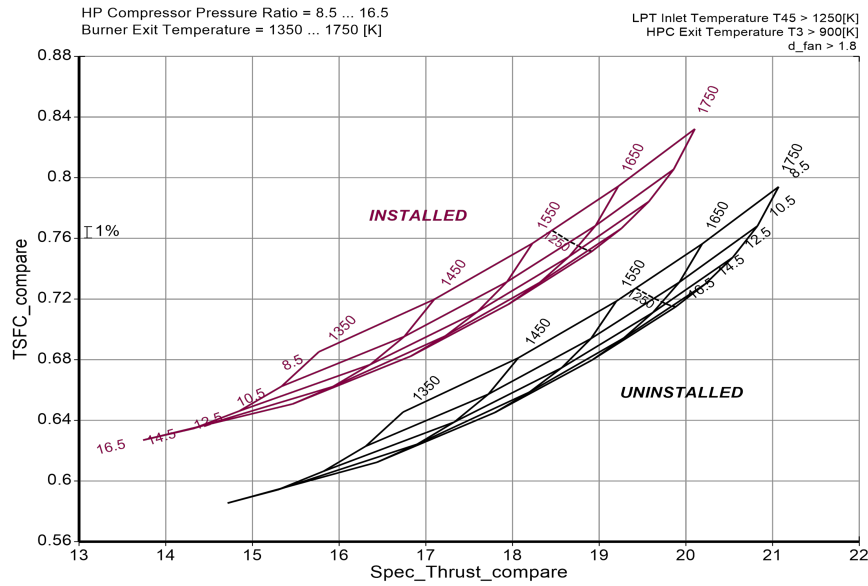


Figure 3.6: A separate exhaust parametric plot comparing the variation in TSFC [kg/hr/-daN] and Specific Thrust [daN/kg/s] with HPCPR and TIT for uninstalled and installed performance.

To explore how installation impacts theoretical performance, the study to produce Figure 3.2 was repeated for installed and uninstalled performance, creating Figure 3.5. Figure 3.5 demonstrated that installation weakens engine performance, as $TSFC$ is increased whilst F_{spec} is decreased. Figure 3.5 showed a pure translation between the two performance maps, as both $TSFC$ and F_{spec} differ from $TSFC_I$ and $F_{spec,I}$ by a subtractive constant – the extra engine thrust required to overcome the nacelle drag and engine weight.

3.1.7 Uniform FPR discussion

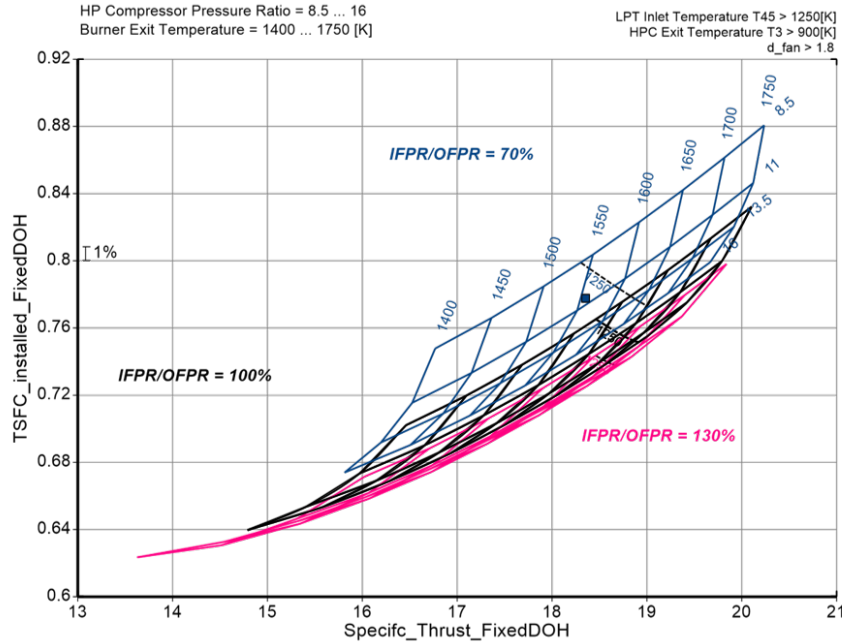


Figure 3.7: A separate exhaust parametric plot comparing the variation in TSFC [kg/hr/-daN] and Specific Thrust [daN/kg/s] with HPCPR and TIT for three different radial pressure distributions.

To explore the validity of matching the inner and outer fan pressure ratio, a short study was completed. Instead of matching IOFP and OFPR in *GASTURB*, the ratio between them was set iteratively to 0.7, 1.0 or 1.3, mimicking a radial-jump of $\pm 30\%$ from hub to tip. The study from Figure 3.2 was repeated for these three testing ratios and plotted as Figure 3.7.

In Figure 3.7 the *TSFC* increased notably for $IFPR > OFPR$ and decreased slightly for $IFPR < OFPR$. However, $IFPR > OFPR$ does not correspond to real behaviour; the tip of the fan blades travel faster than the hub relative to the flow, therefore pressure ratio increases radially (excluding the impact of tip-losses). As such, only $IFPR/OFPR > 1$ was considered, for which there was a small decrease in both *TSFC* and F_{spec} . In Figure 3.7, this offset did not vary significantly throughout the parametric space, implying that any non-uniformity in FPR could be easily accounted for through a simple correction factor. Therefore, the matched FPR condition used in the parametric study was deemed suitable for initial design.

3.1.8 Summary of Selected Design Parameters

Following the parametric study, the engine parameters were selected systematically. Figure 3.1 provided an initial range of BPR and FPR values to be further refined. A value for HPCPR (and hence OPR) was selected using Figure 3.2, in addition to an approximate range for TIT. Figure 3.3 was then used (with reference to the previous studies) to confirm a value of FPR. Finally Figure 3.4 was used to constrain initial estimates for BPR and TIT, whilst Figure 3.5 was used to identified a suitable DOH. Values for OPR,

FPR, BPR, TIT and DoH were then used as inputs to the design point cycle in **GASTURB**, the parameters for which were recorded in Table 3.1.

Table 3.1: Selected design point parameters for the separate-exhaust configuration.

Input Parameter	Value	Units	Output Parameter	Value	Units
BPR	7	-	d_{fan}	1.18	m
FPR	1.65	-	$F_{n,inst}$	12.3	kN
HPCPR	13	-	F_{spec}	13.6	daN/kg/s
IPCPR	1.81	-	TSFC	0.631	kg/hr/daN
TIT	1575	K	W_{engine}	1291	kg
DoH	0.2	-	η_{IPC}	0.928	-
			$\eta_{p, core}$	0.461	-
			$\eta_{p, HPC}$	0.923	-
			$\eta_{p, LPC}$	0.905	-
			$\eta_{p, propulsive}$	0.766	-

3.2 Parametric Study - Mixed Exhaust at Design Point

3.2.1 BPR

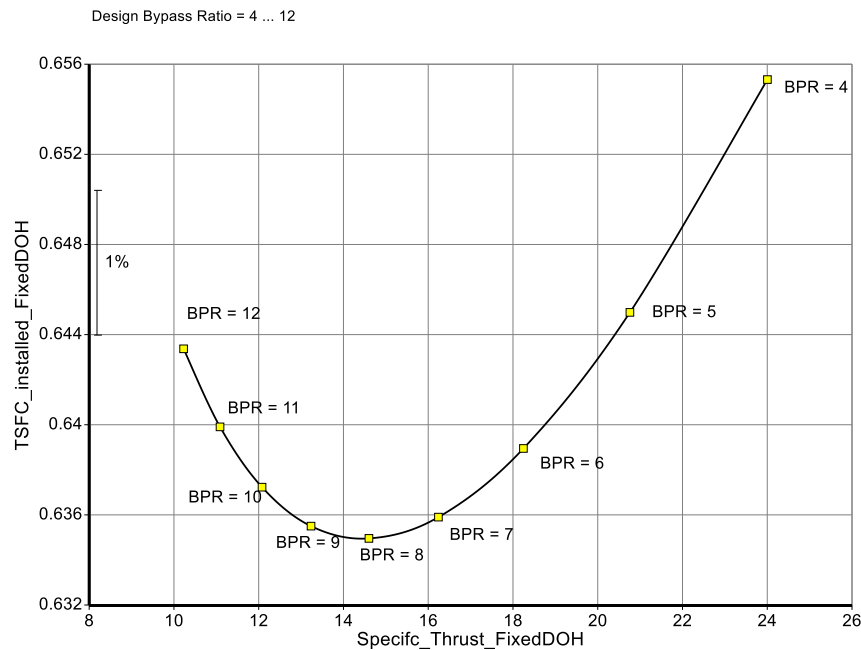


Figure 3.8: A mixed exhaust parametric plot describing the variation in installed TSFC [kg/hr/daN] and installed Specific Thrust [daN/kg/s] with BPR

The relationship between BPR and the installed TSFC and specific thrust was explored in the study and displayed in Figure 3.8. The range of BPR selected was 4-12, with a step size of 1. The figure displayed that increasing BPR causes a decrease in both TSFC and specific thrust until the turning point was reached at a BPR of 8. At a performance level, the bypass ratio represents the ratio of thrust produced by two components - the airflow

through the core duct and the airflow through the bypass duct. As BPR increases, more air passes through the bypass, which means more of the thrust is produced by the slower bypass air instead of the faster core stream air. The specific thrust can be expressed as:

$$F_{spec} = (1 + FAR)V_e - V_0 \quad (3.2)$$

As shown in Equation 3.2, the specific thrust depends directly on the exhaust velocity V_e - as such, the increased airflow through the bypass duct will reduce the exhaust velocity and hence the specific thrust. TSFC also decreases with an increase in BPR - the propulsive efficiency increases as more airflow passes through the bypass duct. This is a result of improved efficiency at lower (average) airflow speeds. The energy transfer within the engine is more effective and the reduced exhaust velocity minimises the kinetic energy losses. This in turn requires a lower mass fuel flow rate to achieve the same level of thrust, reducing TSFC. Past the turning point at $BPR = 8$, the benefits gained by using a lower mass fuel flow are counteracted by design constraints. High BPRs require the fan to compress increasingly large airflows, which, after the turning point, loses efficiency and needs more energy - ultimately this causes an increase in TSFC. From this, the optimal BPR value was chosen to $BPR = 8$, as this minimises TSFC. However, any values within the range 7-9 still produced satisfactory results, so the value had some opportunity to move based on the other parametric studies.

3.2.2 OPR vs TIT

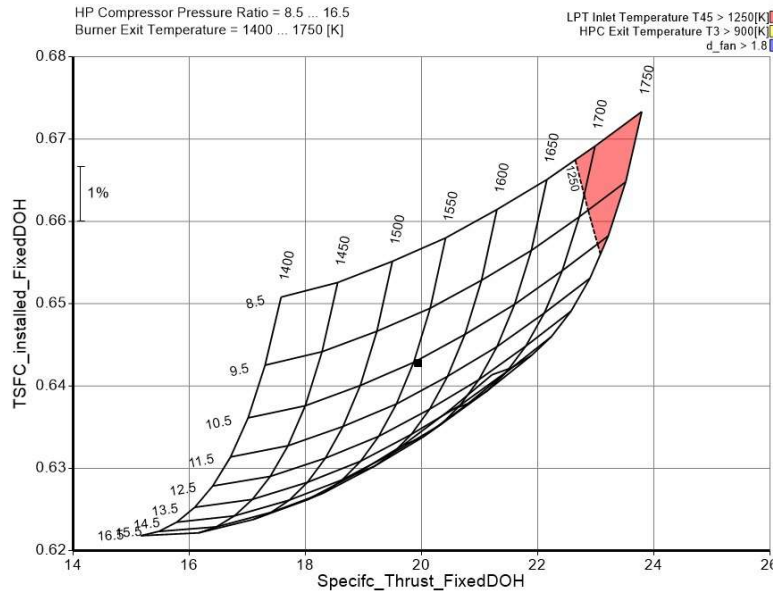


Figure 3.9: A mixed exhaust parametric plot describing the variation in installed TSFC [kg/hr/daN] and installed Specific Thrust [daN/kg/s] with Overall Pressure Ratio (OPR) and Turbine Inlet Temperature (TIT).

Figure 3.9 shows a contour plot that depicts the relationship between a gas turbine engine's specific thrust and TSFC under various operating circumstances. The variables of interest are the HPC pressure ratio and the burner exit temperature. Figure 3.9

illustrates how various factors impact engine performance, with a focus on efficiency and thrust production.

The x-axis shows specific thrust, which is expressed in units of thrust per unit airflow. This is an essential measure that indicates how much thrust an engine can generate for a given volume of air moving through it. The y-axis indicates TSFC, which evaluates fuel efficiency. TSFC is the quantity of fuel used to generate one unit of thrust over time, with lower values indicating higher fuel efficiency. The contour lines on the graph reflect constant values for burner exit temperatures ranging from 1400K to 1750K, as well as HPC pressure ratios ranging from 8.5 to 16.5.

Analysing the overall patterns in the figure reveals a trade-off between particular thrust and TSFC. As specific thrust grows, so does TSFC, indicating that creating greater thrust consumes more fuel, diminishing efficiency. Higher burner exit temperatures often result in higher specific thrusts, but also in higher TSFC, indicating less fuel efficiency. Furthermore, raising the HPC pressure ratio tilts the contours towards larger specific thrusts for a given TSFC. Higher pressure ratios enhance the engine's capacity to compress air, which increases thrust but at the cost of increased fuel consumption.

Figure 3.9 also shows important zones. The red shaded area represents places where the LPT input temperature (T_{45}) surpasses 1250K. Operating in this zone can cause material and thermal stress on turbine components, limiting engine durability. Although not coloured in Figure 3.9, the labels indicate comparable critical zones for HPC exit temperature ($T_3 > 900K$) and fan diameter concerns ($d_{fan} > 1.8$).

3.2.3 FPR vs OPR

A plot of FPR vs OPR was not able to be generated for the mixed exhaust section. In order to accurately model the engine performance in **GASTURB**, the inner and outer fan pressures were matched (for further detail on the **GASTURB** setting view Appendix D). The matching was necessary to ensure that the airflow at fan entry was correct. If the fan pressure ratios are not matched, then airflow separation will occur, which significantly increases drag and reduces efficiency. For further detail on the matching, refer back to Section 3.1.7. For the mixed exhaust, at the point of mixing, the pressures must be equal. This is known as the Kutta condition. In order to achieve this, the pressure in the fan and core ducts were matched - this required iteration on the outer fan pressure ratio. This meant that the outer fan pressure ratio was defined by the Kutta condition, whilst the inner fan pressure ratio was defined by the matching. Hence, for any given design point, only a single FPR value was valid. This meant that FPR was not a design point - it was dependent on the other parameters selected. For further information on FPR for the mixed exhaust, refer to Appendix B. As a plot for FPR vs. OPR was unable to be generated, instead a plot for BPR vs. OPR was created. This is displayed in Figure 3.10. The trend for BPR was consistent with the trend displayed in Figure 3.8 - TSFC and specific thrust decreased with BPR until the turning point was reached. Based on Figure 3.10, the ideal range for BPR was selected as 7-10, which is consistent with the conclusion drawn in Section 3.2.1. Similarly, as OPR increased, TSFC decreased. Increasing OPR increased the thermodynamic efficiency of the engine. A higher pressure ratio increased the efficiency of the combustion chamber - combustion was more complete (CO_2 is the primary carbon product of the combustion reaction). Overall, raising OPR increased the

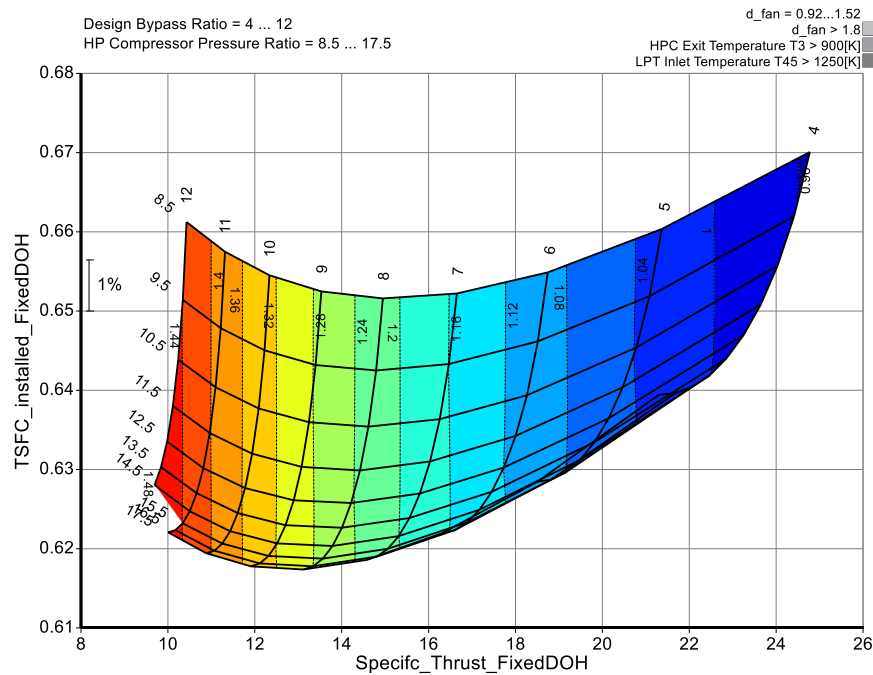


Figure 3.10: A mixed exhaust parametric plot describing the variation in installed TSFC [kg/hr/daN] and installed Specific Thrust [daN/kg/s] with Bypass Ratio (BPR) and Overall Pressure Ratio (OPR)

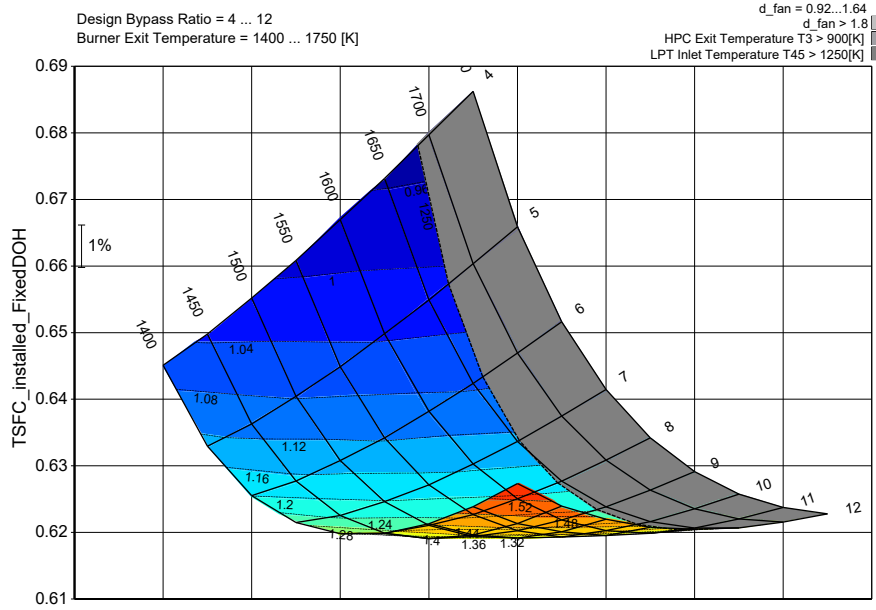
ability of the engine to convert the chemical energy of the fuel into the kinetic energy of the exhaust. Specific thrust was not heavily affected by increasing OPR, although there was a slight trend for it to decrease as OPR increased. As such, the selected range of OPR based on Figure 3.10 was 12.5-17.5, as this minimised TSFC.

3.2.4 BPR vs TIT

In this study, the effects of BPR and TIT were investigated and plotted against TSFC and specific thrust, shown in Figure 3.11. The same result was also plotted with specific thrust on the x-axis, which can be seen in Figure A.3.

Figure 3.11 shows a clear trend of the effects of BPR and TIT on TSFC. For a given low to medium BPR value, the lower the TIT the more efficient the engine becomes, this is due to a smaller FAR ratio required to meet the TIT demand. The thrust was compensated for by a larger fan diameter, hence mass flow rate. However, for higher BPRs the effects of reducing TIT were not nearly as strong, in fact at very high BPRs there was a critical point where further reduction in TIT resulted in a decrease in efficiency.

The result in Figure A.3 highlights the high dependence F_{spec} has on BPR. This is an expected result, the larger the BPR leads to an increase in mass flow and as thrust is iterated to be constant, a higher BPR results in a lower F_{spec} . Along a constant TIT, BPR tends to decrease the TSFC a result that stems from the increase in power drawn from the LPT, leading to a lower V9 and hence a higher propulsive efficiency and therefore lower TSFC. At very high BPR and low TIT there remains a critical point where the TSFC increases, this is due to the power required from the fan being too large for the LPT, hence more fuel is burned to increase the power that can be supplied from the LPT.



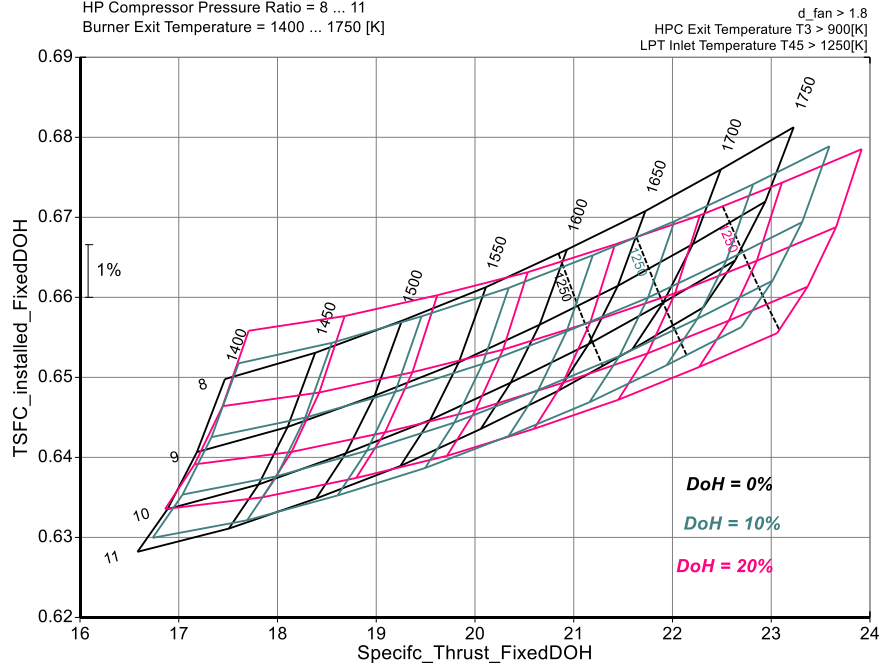


Figure 3.12: A mixed exhaust parametric plot describing the variation in installed TSFC [kg/hr/daN] and installed Specific Thrust [daN/kg/s] with HPCPR and TIT. This was repeated for three fixed-degrees of Hybridisation (DoHs).

$$\begin{aligned}
 (1 + \text{FAR}) (\text{TIT}) \left[1 - \left(\frac{p_{t5}}{p_{t4}} \right)^{\frac{(\gamma-1)\eta_{p,turb}}{\gamma}} \right] &= T_{t2} \left[\text{OPR}^{\left(\frac{\gamma-1}{\gamma\eta_{p,comp}} \right)} - 1 \right] \\
 &+ T_{t2} \left[\text{FPR}^{\left(\frac{\gamma-1}{\gamma\eta_{p,fan}} \right)} - 1 \right] \text{BPR} + \frac{F_N V_0 \text{DoH}}{2(1 - \text{DoH})} \quad (3.4)
 \end{aligned}$$

The hybridisation effect draws power from the LPT to power the electric fan, therefore reduces the power delivered to the bypass fan and hence reduces the OPR. As the other terms on the right-hand side of Equation 3.4 are constant, this means that either the FAR, TIT or LPTPR has to increase so that the equation is satisfied. The most fundamental difference between the separate exhaust and mixed flow is the kutta condition, which fixes $p_{t5} = p_{t25}$. In addition, $p_{t4} \approx p_{t3}$ which is obviously not able to decrease as this would further reduce the OPR. Therefore, for mixed flow, either the TIT or FAR has to increase for a given increase in hybridisation. Figure 3.12 shows the interplay between these two variables to ensure the relationship in Equation 3.4 is satisfied. At low TIT the FAR compensates by increasing; at high TIT the FAR compensates by decreasing. The level of hybridisation dictates how large this compensation is, which explains the more pronounced clockwise rotation at higher levels of hybridisation in Figure 3.12.

Given the TIT design point range of 1500-1600K, it is recommended a DoH of 10% which allows for some gains in efficiency while also much smaller effects if operated at lower TIT values, unlike DoH of 20%.

3.2.6 Installation Effects

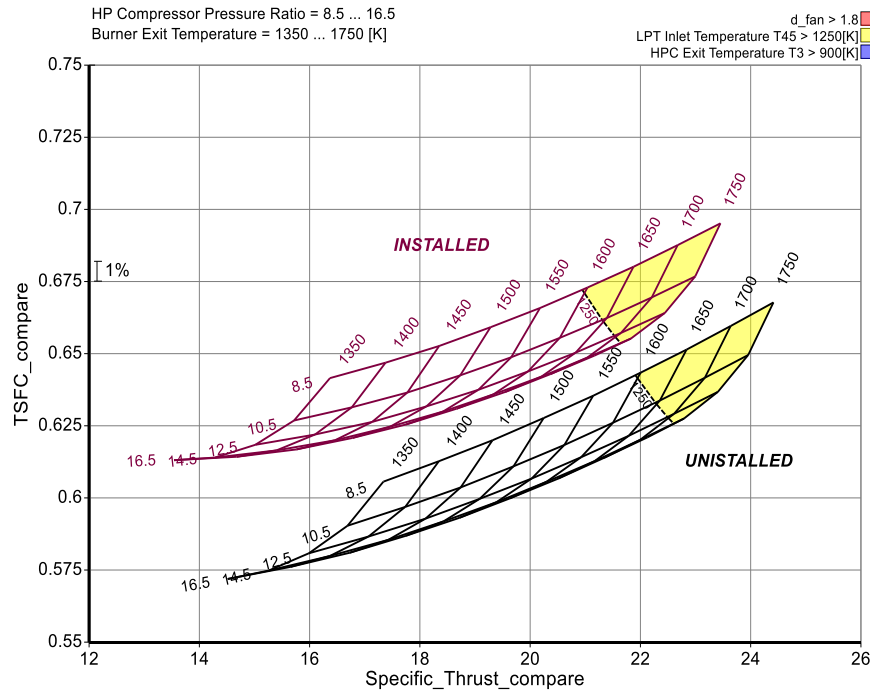


Figure 3.13: A mixed exhaust parametric plot comparing the variation in TSFC [kg/hr/-daN] and Specific Thrust [daN/kg/s] with HPCPR and TIT for uninstalled and installed performance.

Figure 3.13 highlights the installation effects on the TSFC and specific thrust of the engine. The installation effects primarily related to the drag produced by the nacelle of the engine. As BPR was increased, the size of the engine also increased - this increases the size of the nacelle and hence the nacelle drag. Fundamentally, this meant that the engine size was limited by the nacelle drag. Once a sufficiently large engine size was reached, the increase in thrust by raising BPR was counteracted by the increase in nacelle drag. Overall, Figure 3.13 illustrated that the engine performance was reduced when installed, as the increased engine weight and nacelle drag increased the required thrust.

3.2.7 Summary of Selected Design Parameters

Following the mixed exhaust parametric study, the engine parameters were selected. Figure 3.8 outlined the optimal BPR range of 7-9. The BPR range was confirmed in Figure 3.11, which was also used to select a TIT of 1550 as this balanced performance with material limits and tolerance either side. Figure 3.10 was used to determine the HPCPR, which was selected to be 12.5, due to the optimal BPR range and the diminishing returns of further increase. Figure 3.12 showed the effects of hybridisation, in combination with the BPR and TIT, it was discovered that a hybridisation of 10% resulted in a marginal decrease in TSFC, therefore deemed best. Note that the FPR is set for a given OPR due to the kutta condition and is therefore an output for the mixed exhaust study, refer to section B for further discussion on this.

Table 3.2: Selected design point parameters for the mixed-exhaust configuration.

Input Parameter	Value	Units	Output Parameter	Value	Units
BPR	8	-	d_{fan}	1.22	m
HPCPR	12.5	-	$F_{n,inst}$	13.3	kN
IPCPR	1	-	F_{spec}	14.9	daN/kg/s
TIT	1550	K	TSFC	0.67	kg/hr/daN
DoH	0.1	-	W_{engine}	1378	kg
			$\eta_{p, IPC}$	0.950	-
			$\eta_{p, core}$	0.463	-
			$\eta_{p, HPC}$	0.924	-
			$\eta_{p, LPC}$	0.908	-
			$\eta_{p, propulsive}$	0.763	-
			FPR	1.54	-

3.3 Engine Architecture Comparison

The difference between separate and mixed exhaust engines is: in a separate exhaust the core and bypass streams are expelled in separate nozzles, whilst in a mixed exhaust the two streams are combined before being expelled. Typically, a mixed exhaust is more effective as combining the streams leads to a greater thrust efficiency. Based on the studies performed, the difference between the two is small but not insignificant. Both produced fairly similar output parameters, as shown in Tables 3.1 and 3.2. The major difference was in TSFC and engine weight, both in favour of the separate streams. This meant that despite the increased efficiency of the mixed exhaust, its increased weight requirements caused it to have a worse performance under the selected conditions than the separate engine. The separate exhaust also allowed for FPR to be set, which as aforementioned is not permitted for the mixed exhaust. This meant that the separate exhaust has enhanced design space to deal with any additional requirements that may arise later in the design process.

3.4 Sensitivity Study

Table 3.3: Sensitivity study conducted at the selected design point for separate and mixed exhaust engines at cruise

	Separate Exhaust				Mixed Exhaust			
	FPR	TIT	BPR	HPCPR	FPR	TIT	BPR	HPCPR
Unit	[-]	[K]	[-]	[-]	[-]	[K]	[-]	[-]
Design Parameters	1.65	1575	7	13	1.54	1550	8	12.5
Delta (Δ)	0.01	15.5	0.05	0.05	0.01	15.5	0.05	0.05
sNOx [%]	0.12	0	0	0.60	0.86	0.01	0	0.55
$\eta_{propulsive}$ [%]	0	-0.31	0.12	0.07	0	-0.31	0.11	0
η_{core} [%]	0	0.08	-0.02	0.08	0.10	-0.01	-0.01	0.06
$\eta_{p,HPT}$ [%]	0	-0.22	0	-0.06	-0.01	-0.17	0	0
$\eta_{p,LPT}$ [%]	0	0	0	0	0	0	0	0
$\eta_{p,HPC}$ [%]	0	0	0	0	0	0	0	0
$\eta_{p,LPC}$ [%]	0	0	0	-0.18	0	0	0.01	0
TSFC [%]	-0.01	0.31	-0.09	-0.57	-0.11	0.18	-0.04	-0.06
F_{spec} [%]	-0.02	1.43	-0.54	-0.3	-0.02	1.42	-0.51	-0.02
d_{fan} [%]	0.01	-0.66	0.25	0.14	0.01	-0.66	0.24	0.01
W_{engine} [%]	0.02	-1.59	0.61	0.34	0.02	-1.58	0.58	0.02
RCF [%]	0.03	4.55	0	1.3	0.18	5.01	0	0.11
BCF [%]	0.03	4.77	0	1.37	0.18	5.17	0	0.12

Table 3.3 shows how sensitive engine parameters are to variations in the chosen design point for the mixed and separate exhaust. The delta of the design parameters was chosen to be $\approx 1\%$ as this would be the upper limits of tolerance in the manufacturing and testing stage of this type of engine. The trends exhibited were largely the same across both engines. For a change in TIT, RCF and BCF were the most sensitive for both engines. RCF and BCF were the most sensitive to TIT, because it directly increases the temperature of flow entering the HPT and therefore a larger cooling fraction is required to maintain blade temperature specified in section 2.2. The propulsive and core efficiencies were most effected by the TIT, since TIT is directly related to throttle setting and because the thrust was iterated to be constant more throttle than required will reduce efficiency. The FPR had minimal effect in both engines as the largest variation was in sNOx where the effect was still fairly negligible, from this it was concluded the FPR was not a design critical parameter. The BPR had the largest effect on F_{spec} and engine weight for both engines, this was simply due to a larger engine which directly increases the weight and the mass flow of air, hence reducing F_{spec} . The TSFC was shown to go down as less fuel has

to be used to meet the thrust requirement. From the BPR sensitivity, it was concluded that it would be better to be slightly above the specified BPR than below. The HPCPR had a large positive effect on sNOx for both engines. The TSFC was seen to go down for both, which is due to the increase in engine weight. From this study it was concluded the TIT is the most critical parameter in terms of its effects of other parts of the engine, the BPR and HPCPR both have a similar degree of ‘knock-on effect’, however it would be preferable to be slightly above the designed BPR and HPCPR than below. The FPR was concluded not to be a sensitive critical parameter. This conclusion can be used to help direct limited resources in the building and testing phase of the engine to ensure it is as close to the designed performance as possible.

3.5 Final Design Point Selection

The final design point was chosen to be the separate exhaust design point - the parameters are shown in Table 3.4. The engine was intended to be used primarily at cruise for passenger services - as such, the most critical design point was the cruise TSFC. Optimising TSFC minimises the fuel consumption at cruise, reducing operating costs. The difference in TSFC between the two exhaust types was almost 0.04 kg/hr/daN, meaning that switching between the two was a significant difference. The majority of the other performance parameters were similar, with the exception of specific thrust. The mixed exhaust engine had a much larger specific thrust (14.9 to 13.6 daN/kg/s). However, the separate engine also had a lower engine weight and fan diameter, which improved the operation of the engine in off-design conditions. Based on all these factors, the separate engine was considered to be superior and was selected as the ideal engine.

Table 3.4: Selected design point parameters for the final configuration.

Input Parameter	Value	Units	Output Parameter	Value	Units
BPR	7	-	d_{fan}	1.18	m
FPR	1.65	-	$F_{n,inst}$	12.3	kN
HPCPR	13	-	F_{spec}	13.6	daN/kg/s
IPCPR	1.81	-	TSFC	0.631	kg/hr/daN
TIT	1575	K	W_{engine}	1291	kg
DoH	0.2	-	η_{IPC}	0.928	-
			$\eta_{p, core}$	0.461	-
			$\eta_{p, HPC}$	0.923	-
			$\eta_{p, LPC}$	0.905	-
			$\eta_{p, propulsive}$	0.766	-

3.6 Off-Design Performance

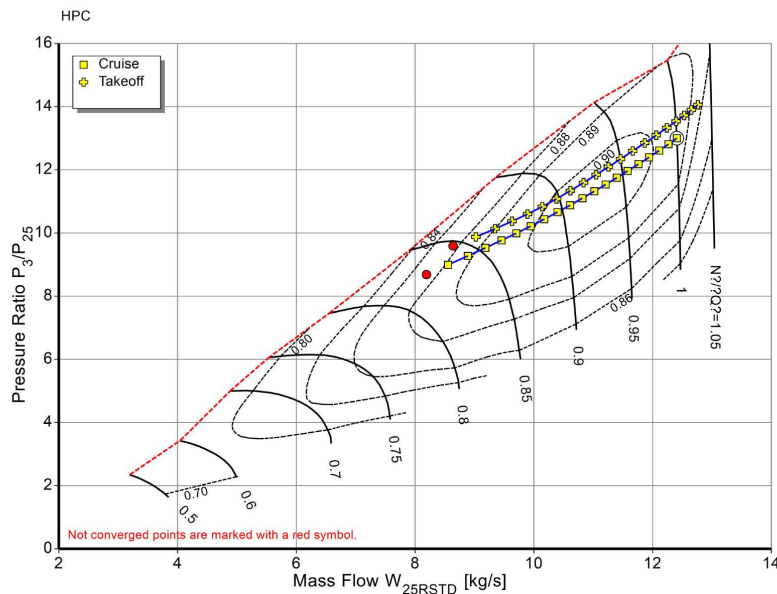


Figure 3.14: The variation in operating line of the HPC at takeoff and cruise

This section examines the selected engine at the off-design point, specifically the take-off situation. The takeoff settings are set at 63 kN thrust per engine at sea level and a Mach number of 0.2. Figure 3.14 shows that the HPC performs similarly at the design and off-design points, with identical pressure ratios. This is due to the HPC's rotor and stator blades, which realign the flow for the next step. As a result of the absence of separation or surge, the pressure ratio between design and off-design locations for a particular RPM will be comparable. As a result, the HPC efficiency remains stable.

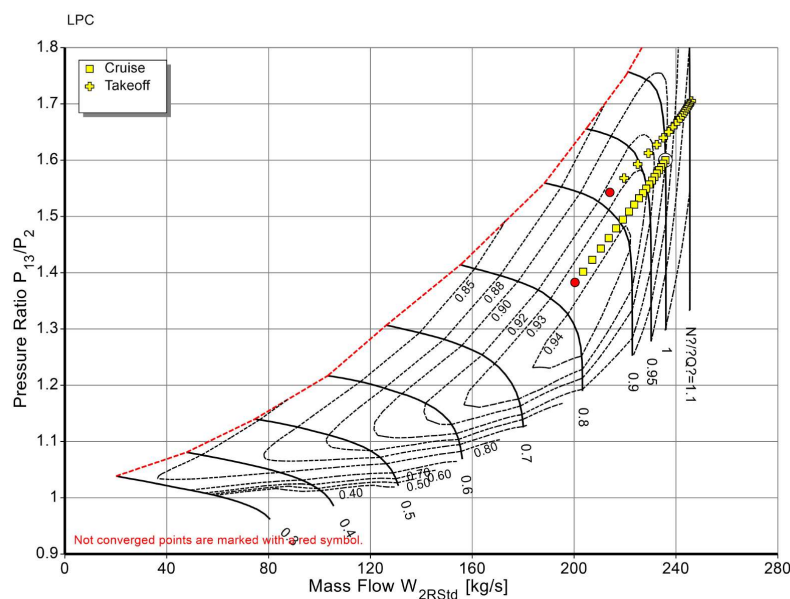


Figure 3.15: The variation in operating line of the LPC at takeoff and cruise

Figure 3.15 shows a contrasting pattern, with the LPC behaving considerably differently at the design and off-design points. Due to the lack of stator blades, the LPC will be more efficient for the design points alone. To correctly interpret figure 3.15, keep in mind that during takeoff, the throttle setting will be as high as possible in order to reduce the distance to takeoff. At cruise, the throttle setting will be somewhat lower, mid to high throttle, around 80 – 90%. Full throttle results in a normalised rotational speed line of 1.1. It can be observed that the LPC has an efficiency of 0.94 for a lower throttle in the cruising setting, as it was built for this flying action, however the LPC has an estimated efficiency of 0.90 during takeoff.

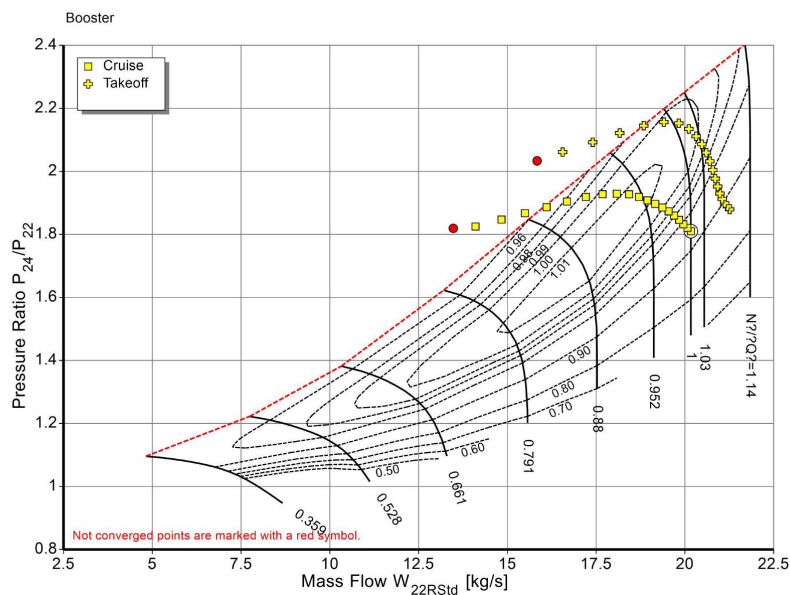


Figure 3.16: The variation in operating line of the booster at takeoff and cruise

The cruise line has a higher positive gradient than the takeoff line due to the limited number of throttle settings. A low throttle setting results in an undesirable pressure ratio, but increasing the throttle leads to a steep increase in the design pressure ratio. A similar approach may be used with the intermediate compressor map. The cruise operating lines lies above the surge line at low RPMs, however this is irrelevant because these RPMs will never be used. There is no possibility of surge at full power during takeoff since a low pressure ratio is achieved. At low mass flow rates, the relative flow vector seen by the compressor blades is too high, posing a surge danger for the design point.

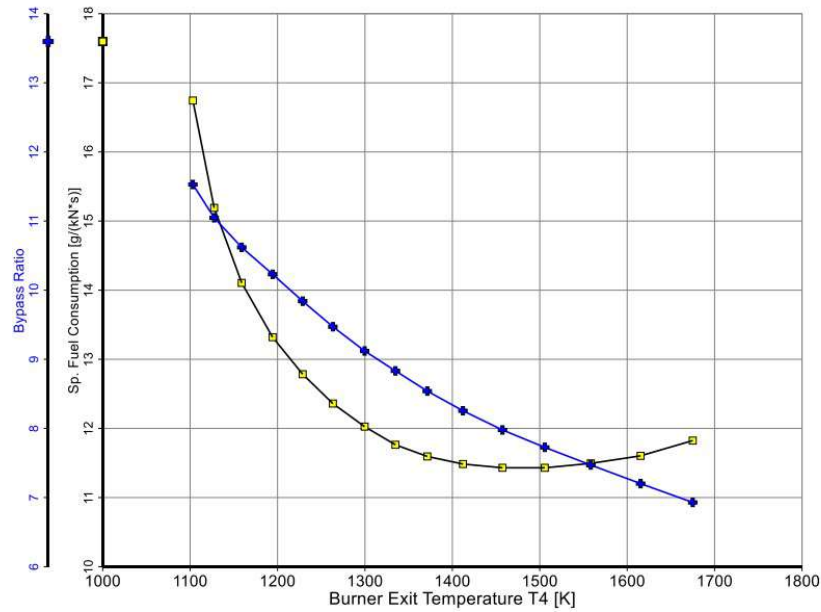


Figure 3.17: The variance in BPR and TSFC with throttle setting.

The thrust required per engine during takeoff is 63 kN. It's worth noting that as altitude climbs, less thrust is produced. This is due to a reduction in air density with height. As air density declines, fewer molecules are present for compression, resulting in less oxygen available for burning, lowering the amount of thrust that may be created. Figure 3.17 shows a clear association between BPR and TSFC in respect to throttle settings. The growing TIT on the x-axis indicates the throttle setting. At low throttle levels, core thrust is restricted, hence the fan is the major thrust supplier, resulting in high BPR. This occurs when the engine generates additional core thrust to increase overall power, resulting in the ideal BPR at the flying state. As smaller increases in thrust need more \dot{m}_f , TSFC is lowered. Because takeoff accounts for a minor amount of operational time, a small TSFC increase is permitted to boost F_{net} .

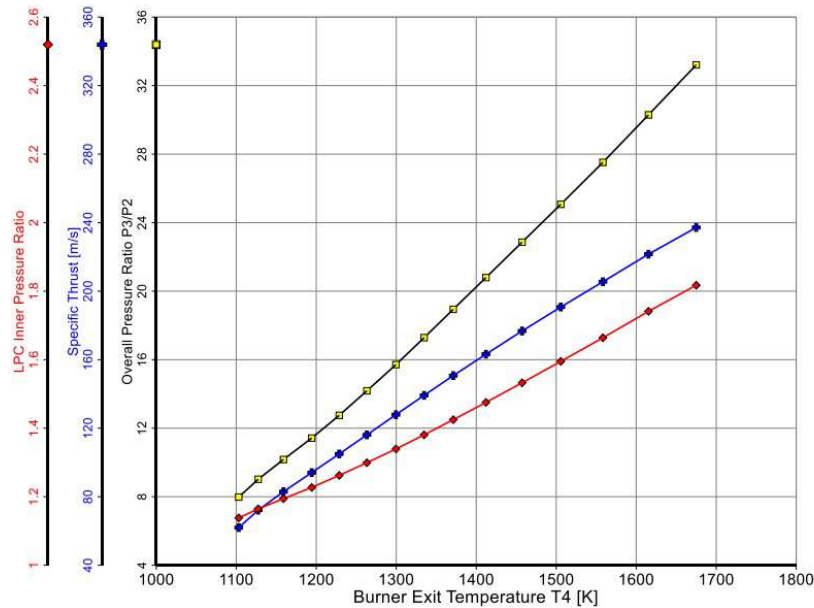


Figure 3.18: The variance in LPR, OPR and specific thrust with throttle settings.

Figure 3.18 shows how LPR, OPR and specific thrust vary with throttle setting. LPR and OPR both rise with throttle setting, when the engine spools up, the compressor RPM increases, resulting in increased fan and overall pressure. Increased pressure allows for greater energy extraction from the air-fuel combination, resulting in higher specific thrust with less air mass flow.

4 Conclusion

In summary, the ideal engine for the design brief is a separate exhaust turbofan with 20% DoH, as conveyed in Table 3.1. The deciding benefit of the separate configuration was the notable difference in TSFC and engine weight portrayed by the studies. Whilst, the selection of an engine with hybridisation was due to the greater efficiency observed with an increased DoH. Hence, the report successfully evaluated separate and mixed turbofan engines across various configurations to ascertain the optimum layout for the design brief.

References

- [1] AIAA Foundation, *A hybrid-electric propulsion system using fuselage boundary layer ingestion for a single-aisle commercial aircraft*, AIAA Foundation Student Design Competition 2022/23, Undergraduate Team - Engine, 2022. [Online]. Available: <https://www.aiaa.org>.
- [2] T. Okura, “Materials for aircraft engines,” University of Colorado Boulder, Tech. Rep., 2015. [Online]. Available: https://www.colorado.edu/faculty/kantha/sites/default/files/attached-files/73549-116619_-_takehiro_okura_-_dec_17_2015_1027_am_-_asen_5063_2015_final_report_okura.pdf.
- [3] I. Halliwell *et al.*, “Materials for aircraft engines,” AIAA, Tech. Rep., 2022. [Online]. Available: https://www.aiaa.org/docs/default-source/uploadedfiles/membership-and-communities/university-students/design-competitions/rfp---a-hybrid-electric-propulsion-system-for-a-single-aisle-commercial-aircraft_final-85.pdf.
- [4] N. Meier. “Civil turbofan specifications.” Accessed: 2024-05-12. (2024), [Online]. Available: <https://jet-engine.net/civtfspec.htm>.
- [5] D. Verstraete, *Aerospace Propulsion: AERO3261*. USYD Aero, 2013.

A Supporting Figures

A.1 Separate Exhaust Study

A.1.1 OPR vs TIT

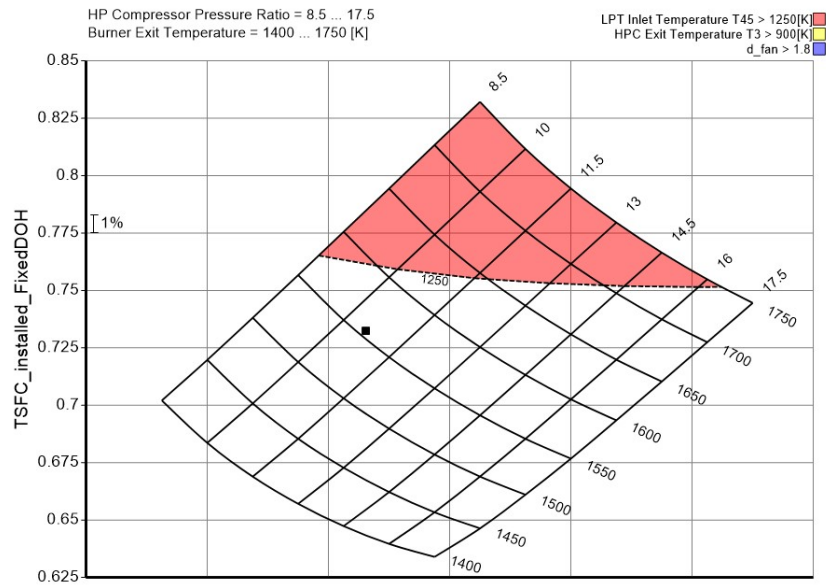


Figure A.1: A separate exhaust parametric plot describing the variation in installed TSFC [kg/hr/daN] and installed Specific Thrust [daN/kg/s] with Overall Pressure Ratio (OPR) and Turbine Inlet Temperature (TIT). This was plotted from the side wherein F_{spec} was aligned into the page.

A.1.2 BPR vs TIT

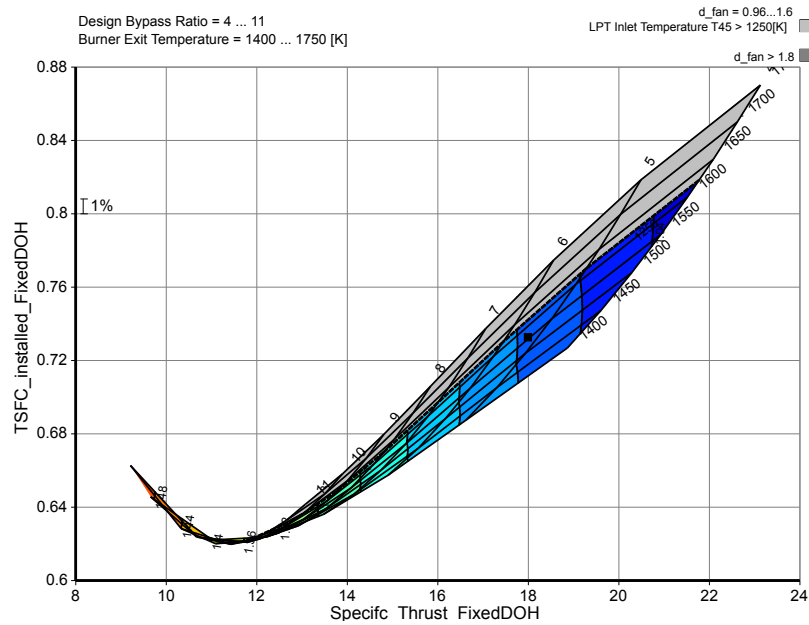


Figure A.2: A separate exhaust parametric plot describing the variation in installed TSFC [kg/hr/daN] and installed Specific Thrust [daN/kg/s] with Bypass Ratio (BPR) and Turbine Inlet Temperature (TIT) in a standard view.

A.2 Mixed Exhaust Study

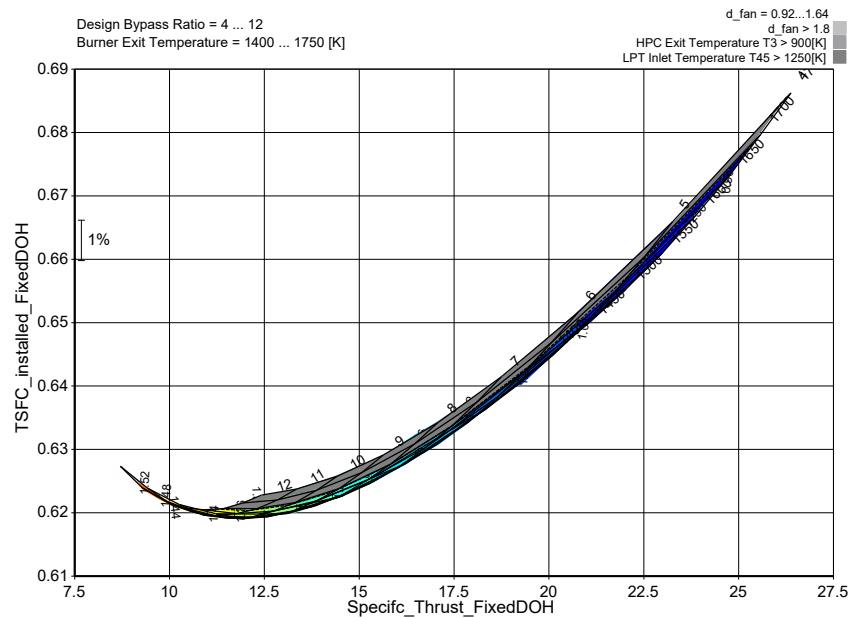


Figure A.3: A mixed exhaust parametric plot describing the variation in installed TSFC [kg/hr/daN] and installed Specific Thrust [daN/kg/s] with Bypass Ratio (BPR) and Turbine Inlet Temperature (TIT) in standard view.

B Mixed Fan Pressure Ratio Notes

B.1 Figures

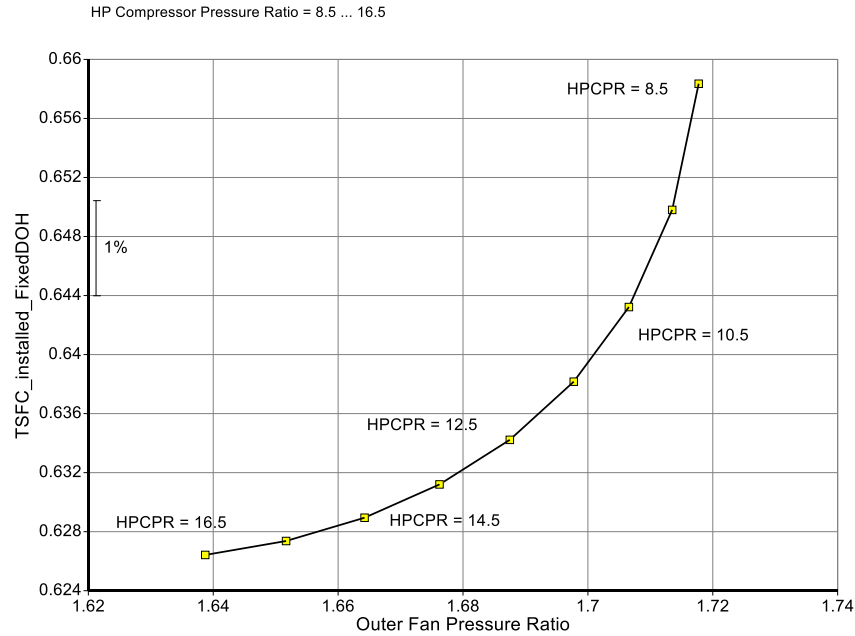


Figure B.1: A mixed exhaust parametric plot describing the variation in installed TSFC [kg/hr/daN] and Fan Pressure Ratio with Overall Pressure Ratio (OPR)

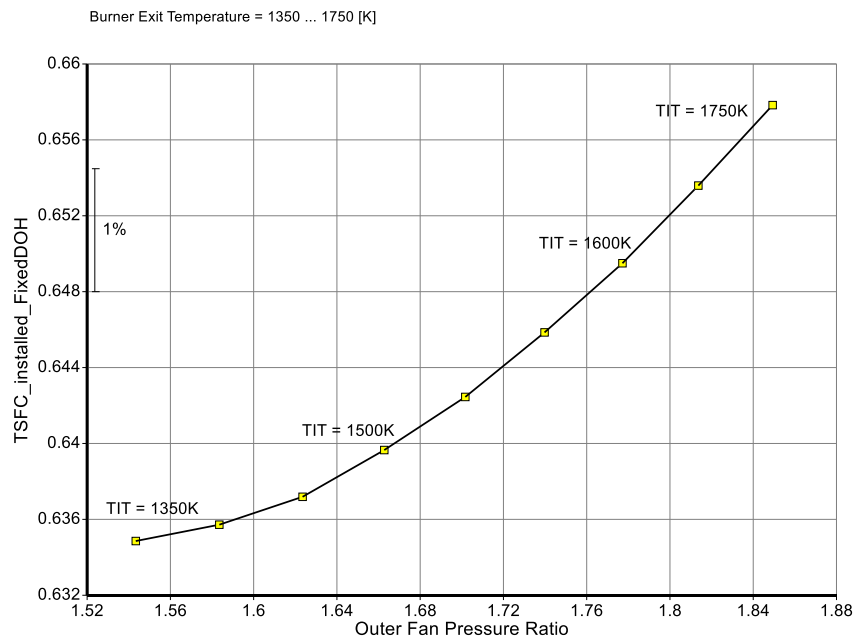


Figure B.2: A mixed exhaust parametric plot describing the variation in installed TSFC [kg/hr/daN] and Fan Pressure Ratio with Turbine Inlet Temperature (TIT) [K]

B.2 Discussion

Figures B.1 and B.2 display the effect of changing OPR and TIT on FPR. The figures show that there was a limited change in FPR with these parameters and that there was a corresponding change in TSFC, which represented the change in TSFC with FPR. However, it is disingenuous to consider the change in FPR with TSFC as a design parameter - for the mixed exhaust, as discussed in Section 3.2.3, FPR is fixed by the other parameters selected. Hence FPR functions as an output of the design parameters inputs, and so should not be considered as a design parameter for the mixed exhaust.

C GASTURB for Separate

C.1 Iteration Parameters

Variable	min	max	Target	Value
Polytr.Inner LPC Efficiency	0.7	1	IterLPCIn_PolyEff=E221polPolyE	1
Polytr.Outer LPC Efficiency	0.7	1	IterLPCOut_PolyEff=E213polPoly	1
Inner Fan Pressure Ratio	1	10	IterFanRatio=ZP21q2/ZP13q2	1
Polytr.IPC Efficiency	0.7	1	IterPC_PolyEff=E2224polPolyEf	1
Polytr.HPC Efficiency	0.7	1	IterHPC_PolyEff=E253polPolyEff	1
HPT NGV 1 Cooling Air / W25	0	0.3	IterNGV=CoolFrNGV-WCHN1q25	0
HPT Rotor 1 Cooling Air / W25	0	0.3	IterRot=CoolFrRotor-WCHR1q25	0
HPT NGV 2 Cooling Air / W25	0	0.3	IterNGV2=CoolFrNGV-WCHN2q25	0
HPT Rotor 2 Cooling Air / W25	0	0.3	IterRot2=CoolFrRotor-WCHR2q25	0
Inlet Corr. Flow W2Rstd	0	1000	Total_Thrust_fixed=F_fan_fixed+FN*2	30.2
Power Offtake	0	1000	PWX_fixed_iter=PWX-Power_Outake_DOH_fixed	0
Polytr.HPT Efficiency	0.7	1	IterHPT_PolyEff=E444polPolyEff_HPT_corrected	1

Figure C.1: Iteration variables in for separate exhaust GASTURB window.

C.2 Composed Variables

```

cp_val1: COOLING_PARAMETERS_APPENDIX_B=1 // *****
cp_val2: T_metal=1250 // Metal Temperature
cp_val3: epsNGV=(T4_D-T_metal)/(T4_D-T3) // Epsilon NGV
cp_val4: epsRotor=(T41-T_metal)/(T41-T3) // Epsilon Rotor
cp_val5: CoolFrNGV=0.06*epsNGV/(1-epsNGV) // Cooling Fraction of NGV
cp_val6: CoolFrRotor=0.06*epsRotor/(1-epsRotor) // Cooling Fraction of
Rotor
cp_val7: IterNGV=CoolFrNGV-WCHN1q25 // Iteration Variable for NGV 1
Cooling (Target = 0)
cp_val8: IterRot=CoolFrRotor-WCHR1q25 // Iteration Variable for Rotor
1 Cooling (Target = 0)
cp_val9: IterNGV2=CoolFrNGV-WCHN2q25 // Iteration Variable for NGV 2
Cooling (Target = 0)
cp_val10: IterRot2=CoolFrRotor-WCHR2q25 // Iteration Variable for
Rotor 2 Cooling (Target = 0)
cp_val11: POLYTROPIC_EFFICIENCY_APPENDIX_B=1 //
*****
cp_val12: PolyEff_HPT_corrected=0.8679-CoolFrNGV // HPT Efficiency
reduced with cooling fraction correction
cp_val13: IterHPT_PolyEff=E444pol/PolyEff_HPT_corrected // Iteration
Variable for HPT Polytropic Efficiency (Target = 1)
cp_val14: n_stag_LPC=1 // Number of Fan Stages
cp_val15: n_stag_IPC=3 // Number of Booster Stages
cp_val16: n_stag_HPC=9 // Number of HPC Stages

```

```

cp_val17: PiCstagLPC=ZP13q2^(1/n_stag_LPC) // Stage Pressure Ratio of
Fan
cp_val18: PiCstagIPC=ZP24q22^(1/n_stag_IPC) // Stage Pressure Ratio of
Booster
cp_val19: PiCstagHPC=ZP3q25^(1/n_stag_HPC) // Stage Pressure Ratio of
HPC
cp_val20: IterFanRatio=ZP21q2/ZP13q2 // Iteration Variable for Inner
and Outer Fan Matching (Target = 1)
cp_val21: PolyEffLPC=(-1/30)*PiCstagLPC+24/25 // Polytropic Efficiency
of Fan
cp_val22: PolyEffIPC=(-1/10)*PiCstagIPC+21/20 // Polytropic Efficiency
of Booster
cp_val23: PolyEffHPC=(-2/15)*PiCstagHPC+11/10 // Polytropic Efficiency
of HPC
cp_val24: IterLPCin_PolyEff=E221pol/PolyEffLPC // Iteration Variable
for LPC (inner) Polytropic Efficiency (Target = 1)
cp_val25: IterLPCout_PolyEff=E213pol/PolyEffLPC // Iteration Variable
for LPC (outer) Polytropic Efficiency (Target = 1)
cp_val26: IterIPC_PolyEff=E2224pol/PolyEffIPC // Iteration Variable
for IPC Polytropic Efficiency (Target = 1)
cp_val27: IterHPC_PolyEff=E253pol/PolyEffHPC // Iteration Variable for
HPC Polytropic Efficiency (Target = 1)
cp_val28: INSTALLATION_EFFECTS=1 // *****
cp_val29: kutta=St16_P/St6_P // Kutta Condition (Target = 1)
cp_val30: NACELLE_DRAG=1 // *****
cp_val31: k_var=0.04 // Constant
cp_val32: NThrust=FN // FN is given in kN
cp_val33: Dnac=k_var*V0*(FN/FNqW2) // Nacelle drag
cp_val34: Fnet_eff=NThrust*(1-k_var*V0/FNqW2) // FN effective
cp_val35: MTOW=60160 // MTOW
cp_val36: Area=W2/(rho0*V0) // Area that air passes through
cp_val37: d_fan=(4*Area/3.1415/((1-0.3^2))^0.5 // Diameter of fan
cp_val38: W_engine=860*d_fan^2.4 // Engine weight
cp_val39: Fnet_installed=Fnet_eff-(W_engine/(MTOW*0.95/Dnac)) // FN
CORRECTED
cp_val40: TSFC_installed=(WF/Fnet_installed)*36 // TSFC corrected
cp_val41: FIXED_DOH=1 // *****
cp_val42: P_propulsive=FN*V0 // Propulsive power
cp_val43: DoH_fixed=0.2 // Fixed degree of hybridisation
cp_val44: P_ex_fixed=DoH_fixed*P_propulsive/(1-DoH_fixed) // Power
extracted from fan
cp_val45: FanEff=0.585 // Fan efficiency
cp_val46: F_fan_fixed=FanEff*P_ex_fixed/V0*2 // Thrust produced by fan
cp_val47: Total_Thrust_fixed=F_fan_fixed+FN*2 // Total thrust produced
cp_val48: TSFC_fixed=(WF/Total_Thrust_fixed)*36/2 // TSFC in daN/kg/hr
cp_val49: Power_Outake_DOH_fixed=111.8+P_ex_fixed // Power offtake
cp_val50: PWX_fixed_Iter=PWX-Power_Outake_DOH_fixed // Total power
offtake (Target = 0)
cp_val51: INSTALL_AND_FAN_EFFECTS=1 // *****
cp_val52: F_specific_installed=(Fnet_installed*100)/W2 // Specific
Thrust in daNs/kg
cp_val53: Fixed_TSFC_installed=WF/(Fnet_installed+F_fan_fixed/2)*36 //
TSFC in daN/kg/hr
cp_val54: Fixed_Specific_Thrust=((Fnet_installed+F_fan_fixed/2)*100)/W2
// Specific Thrust in daNs/kg
cp_val55: ZP3q25 // HP comp ratio
cp_val56: ZP13q2 // Outer fan ratio

```

C.3 Design Point Cycle

W	T	P	WRstd						
Station	kg/s	K	kPa	kg/s	FN	=	13.17		
kN									
amb		218.81	23.842		TSFC	=	18.9499		
g/(kN*s)									
2	90.350	246.88	35.990	235.444	WF	=	0.2496		
kg/s									
13	79.056	289.22	59.384	135.142	s NOX	=	0.5534		
21	11.294	289.22	59.384	19.306					
22	11.294	289.22	58.790	19.501	Core Eff	=	0.4606		
24	11.294	347.03	106.411	11.802	Prop Eff	=	0.7663		
25	11.294	347.03	104.283	12.043	BPR	=	7.0000		
3	11.068	749.09	1355.673	1.334	P2/P1	=	0.9900		
31	10.230	749.09	1355.673		P3/P2	=	37.67		
4	10.479	1575.00	1301.446	1.907	P5/P2	=	1.3327		
41	10.919	1544.56	1301.446	1.968					
43	10.919	1127.59	252.918		P16/P6	=	1.26387		
44	11.318	1115.20	252.918		P16/P2	=	1.61700		
45	11.487	1108.14	247.859	9.209	P6/P5	=	0.96000		
49	11.487	769.45	47.965		A8	=	0.17773		
5	11.543	768.81	47.965	39.831	A18	=	0.58559		
8	11.543	768.81	46.046	41.491	XM8	=	1.00000		
18	79.056	289.22	58.197	137.900	XM18	=	1.00000		
Bleed	0.000	749.09	1355.673		WBld/W2	=	0.00000		
-----					CD8	=	0.97976		
Efficiency	isent	polytr	RNI	P/P	CD18	=	0.97600		
Outer LPC	0.8980	0.9050	0.426	1.650	PWX	=	893.4		
Inner LPC	0.8980	0.9050	0.426	1.650	V18/V8,id	=	0.69938		
IP Compressor	0.9219	0.9281	0.578	1.810	WBLD/W22	=	0.00000		
HP Compressor	0.8928	0.9227	0.825	13.000	Wreci/W25	=	0.00000		
Burner	0.9995			0.960	Loading	=	100.00		
HP Turbine	0.8550	0.8290	1.806	5.146	WCHN/W25	=	0.03893		
LP Turbine	0.9174	0.9000	0.504	5.167	WCHR/W25	=	0.03528		
-----					WCLN/W25	=	0.01500		
HP Spool mech Eff	0.9900	Nom Spd	18931 rpm		WCLR/W25	=	0.00500		
LP Spool mech Eff	0.9900	Nom Spd	4000 rpm		WBLD/W25	=	0.00000		
-----					P6/P5	=	0.96000		
P22/P21=0.9900	P25/P24=0.9800	P45/P44=0.9800			P16/P13	=	0.9800		

hum [%]	war0	FHV	Fuel						
0.0	0.00000	43.153	Generic						
Composed Values:									
1: COOLING_PARAMETERS_APPENDIX_B									
= 1 *****									
2: T_metal									
= 1250 Metal Temperature									
3: epsNGV									
= 0.393507 Epsilon NGV									
4: epsRotor									
= 0.370296 Epsilon Rotor									
5: CoolFrNGV									
= 0.0389294 Cooling Fraction of NGV									
6: CoolFrRotor									
= 0.0352828 Cooling Fraction of Rotor									

```

7: IterNGV
  = 0          Iteration Variable for NGV 1 Cooling (Target = 0)
8: IterRot
  = 0          Iteration Variable for Rotor 1 Cooling (Target = 0)
9: IterNGV2
  = 0          Iteration Variable for NGV 2 Cooling (Target = 0)
10: IterRot2
  = 0          Iteration Variable for Rotor 2 Cooling (Target = 0)
11: POLYTROPIC_EFFICIENCY_APPENDIX_B
  = 1          *****
12: PolyEff_HPT_corrected
  = 0.828971   HPT Efficiency reduced with cooling fraction
               correction
13: IterHPT_PolyEff
  = 1          Iteration Variable for HPT Polytropic Efficiency (
               Target = 1)
14: n_stag_LPC
  = 1          Number of Fan Stages
15: n_stag_IPC
  = 3          Number of Booster Stages
16: n_stag_HPC
  = 9          Number of HPC Stages
17: PiCstagLPC
  = 1.65       Stage Pressure Ratio of Fan
18: PiCstagIPC
  = 1.21869    Stage Pressure Ratio of Booster
19: PiCstagHPC
  = 1.32975    Stage Pressure Ratio of HPC
20: IterFanRatio
  = 1          Iteration Variable for Inner and Outer Fan Matching (
               Target = 1...)
21: PolyEffLPC
  = 0.905      Polytropic Efficiency of Fan
22: PolyEffIPC
  = 0.928131   Polytropic Efficiency of Booster
23: PolyEffHPC
  = 0.922699   Polytropic Efficiency of HPC
24: IterLPCin_PolyEff
  = 1          Iteration Variable for LPC (inner) Polytropic
               Efficiency (Target...)
25: IterLPCout_PolyEff
  = 1          Iteration Variable for LPC (outer) Polytropic
               Efficiency (Target...)
26: IterIPC_PolyEff
  = 1          Iteration Variable for IPC Polytropic Efficiency (
               Target = 1)
27: IterHPC_PolyEff
  = 1          Iteration Variable for HPC Polytropic Efficiency (
               Target = 1)
28: INSTALLATION_EFFECTS
  = 1          *****
29: kutta
  = 1.26387    Kutta Condition (Target = 1)
30: NACELLE_DRAG
  = 1          *****
31: k_var
  = 0.04       Constant
32: NThrust

```



```

    = 13.1734    FN is given in kN
33: Dnac
    = 0.857657   Nacelle drag
34: Fnet_eff
    = 12.3157    FN effective
35: MTOW
    = 60160      MTOW
36: Area
    = 1.00294    Area that air passes through
37: d_fan
    = 1.18462    Diameter of fan
38: W_engine
    = 1291.48    Engine weight
39: Fnet_installed
    = 12.2964    FN CORRECTED
40: TSFC_installed
    = 0.730853   TSFC corrected
41: FIXED_DOH
    = 1          *****
42: P_propulsive
    = 3126.24    Propulsive power
43: DoH_fixed
    = 0.2        Fixed degree of hybridisation
44: P_ex_fixed
    = 781.561    Power extracted from fan
45: FanEff
    = 0.585      Fan efficiency
46: F_fan_fixed
    = 3.85322    Thrust produced by fan
47: Total_Thrust_fixed
    = 30.2       Total thrust produced
48: TSFC_fixed
    = 0.148789   TSFC in daN/kg/hr
49: Power_Outake_DOH_fixed
    = 893.361    Power offtake
50: PWX_fixed_Iter
    = 7.28116E-07 Total power offtake (Target = 0)
51: INSTALL_AND_FAN_EFFECTS
    = 1          *****
52: F_specific_installed
    = 13.6097    Specific Thrust in daNs/kg
53: Fixed_TSFC_installed
    = 0.631853   TSFC in daN/kg/hr
54: Fixed_Specific_Thrust
    = 15.7421    Specific Thrust in daNs/kg
55: ZP3q25
    = 13         HP comp ratio
56: ZP13q2
    = 1.65       Outer fan ratio

```

Iteration converged after 18 loops.

Iteration Variables:

1: Polytr.Inner LPC Efficiency (0.7...1)	= 0.905
2: Polytr.Outer LPC Efficiency (0.7...1)	= 0.905
3: Inner Fan Pressure Ratio (1...10)	= 1.65
4: Polytr.IPC Efficiency (0.7...1)	= 0.928131
5: Polytr.HPC Efficiency (0.7...1)	= 0.922699

6:	HPT NGV 1 Cooling Air / W25 (0...0.3)	= 0.0389294
7:	HPT Rotor 1 Cooling Air / W25 (0...0.3)	= 0.0352828
8:	HPT NGV 2 Cooling Air / W25 (0...0.3)	= 0.0389294
9:	HPT Rotor 2 Cooling Air / W25 (0...0.3)	= 0.0352828
10:	Inlet Corr. Flow W2Rstd kg/s (0...1000)	= 235.444
11:	Power Offtake kW (0...1000)	= 893.361
12:	Polytr.HPT Efficiency (0.7...1)	= 0.828971
Iteration Targets:		
1:	cp_val24	= 1
2:	cp_val25	= 1
3:	cp_val20	= 1
4:	cp_val26	= 1
5:	cp_val27	= 1
6:	cp_val7	= 0
7:	cp_val8	= 0
8:	cp_val9	= 0
9:	cp_val10	= 0
10:	cp_val47	= 30.2
11:	cp_val50	= 0
12:	cp_val13	= 1

D GASTURB for Mixed

D.1 Iteration Parameters

Variable	min	max	Target	Value	act
Polytr.Inner LPC Efficiency	0.7	1	IterLPCIn_PolyEff=E221pol/PolyE	1	✓
Polytr.Outer LPC Efficiency	0.7	1	IterLPCOut_PolyEff=E213pol/Poly	1	✓
Inner Fan Pressure Ratio	1	10	IterFanRatio=ZP21q2/ZP13q2	1	✓
Polytr.IPC Efficiency	0.7	1	IterIPC_PolyEff=E2224pol/PolyEf	1	✓
Polytr.HPC Efficiency	0.7	1	IterHPC_PolyEff=E253pol/PolyEff	1	✓
HPT NGV 1 Cooling Air / W25	0	0.3	IterNGV=CoolFrNGV-WCHN1q25	0	✓
HPT Rotor 1 Cooling Air / W25	0	0.3	IterRot=CoolFrRotor-WCHR1q25	0	✓
HPT NGV 2 Cooling Air / W25	0	0.3	IterNGV2=CoolFrNGV-WCHN2q25	0	✓
HPT Rotor 2 Cooling Air / W25	0	0.3	IterRot2=CoolFrRotor-WCHR2q25	0	✓
Inlet Corr. Flow W2Rstd	0	1000	Total_Thrust_fixed=F_fan_fixed+	30.2	✓
Power Offtake	0	1000	PWX_fixed_iter=PWX-Power_Outake	0	✓
Polytr.HPT Efficiency	0.7	1	IterHPT_PolyEff=E444pol/PolyEff	1	✓
Outer Fan Pressure Ratio	1	10	kutta=St16_P/St6_P	1	✓

Figure D.1: Iteration variables in for mixed exhaust GASTURB window.

D.2 Composed Variables

Composed Values for Cycle Design	
cp_val1:	COOLING_PARAMETERS_APPENDIX_B=1 // *****
cp_val2:	T_metal=1250 // Metal Temperature
cp_val3:	epsNGV=(T4_D-T_metal)/(T4_D-T3) // Epsilon NGV
cp_val4:	epsRotor=(T41-T_metal)/(T41-T3) // Epsilon Rotor
cp_val5:	CoolFrNGV=0.06*epsNGV/(1-epsNGV) // Cooling Fraction of NGV
cp_val6:	CoolFrRotor=0.06*epsRotor/(1-epsRotor) // Cooling Fraction of Rotor

```

cp_val7: IterNGV=CoolFrNGV-WCHN1q25 // Iteration Variable for NGV 1
Cooling (Target = 0)
cp_val8: IterRot=CoolFrRotor-WCHR1q25 // Iteration Variable for Rotor
1 Cooling (Target = 0)
cp_val9: IterNGV2=CoolFrNGV-WCHN2q25 // Iteration Variable for NGV 2
Cooling (Target = 0)
cp_val10: IterRot2=CoolFrRotor-WCHR2q25 // Iteration Variable for
Rotor 2 Cooling (Target = 0)
cp_val11: POLYTROPIC_EFFICIENCY_APPENDIX_B=1 //
*****
cp_val12: PolyEff_HPT_corrected=0.8679-CoolFrNGV // HPT Efficiency
reduced with cooling fraction correction
cp_val13: IterHPT_PolyEff=E444pol/PolyEff_HPT_corrected // Iteration
Variable for HPT Polytropic Efficiency (Target = 1)
cp_val14: n_stag_LPC=1 // Number of Fan Stages
cp_val15: n_stag_IPC=3 // Number of Booster Stages
cp_val16: n_stag_HPC=9 // Number of HPC Stages
cp_val17: PiCstagLPC=ZP13q2^(1/n_stag_LPC) // Stage Pressure Ratio of
Fan
cp_val18: PiCstagIPC=ZP24q22^(1/n_stag_IPC) // Stage Pressure Ratio of
Booster
cp_val19: PiCstagHPC=ZP3q25^(1/n_stag_HPC) // Stage Pressure Ratio of
HPC
cp_val20: IterFanRatio=ZP21q2/ZP13q2 // Iteration Variable for Inner
and Outer Fan Matching (Target = 1)
cp_val21: PolyEffLPC=(-1/30)*PiCstagLPC+24/25 // Polytropic Efficiency
of Fan
cp_val22: PolyEffIPC=(-1/10)*PiCstagIPC+21/20 // Polytropic Efficiency
of Booster
cp_val23: PolyEffHPC=(-2/15)*PiCstagHPC+11/10 // Polytropic Efficiency
of HPC
cp_val24: IterLPCin_PolyEff=E221pol/PolyEffLPC // Iteration Variable
for LPC (inner) Polytropic Efficiency (Target = 1)
cp_val25: IterLPCout_PolyEff=E213pol/PolyEffLPC // Iteration Variable
for LPC (outer) Polytropic Efficiency (Target = 1)
cp_val26: IterIPC_PolyEff=E2224pol/PolyEffIPC // Iteration Variable
for IPC Polytropic Efficiency (Target = 1)
cp_val27: IterHPC_PolyEff=E253pol/PolyEffHPC // Iteration Variable for
HPC Polytropic Efficiency (Target = 1)
cp_val28: INSTALLATION_EFFECTS=1 // *****
cp_val29: kutta=St16_P/St6_P // Kutta Condition (Target = 1)
cp_val30: NACELLE_DRAG=1 // *****
cp_val31: k_var=0.04 // Constant
cp_val32: NThrust=FN // FN is given in kN
cp_val33: Dnac=k_var*V0*(FN/FNqW2) // Nacelle drag
cp_val34: Fnet_eff=NThrust*(1-k_var*V0/FNqW2) // FN effective
cp_val35: MTOW=60160 // MTOW
cp_val36: Area=W2/(rho0*V0) // Area that air passes through
cp_val37: d_fan=(4*Area/3.1415/((1-0.3^2))^0.5 // Diameter of fan
cp_val38: W_engine=860*d_fan^2.4 // Engine weight
cp_val39: Fnet_installed=Fnet_eff-(W_engine/(MTOW*0.95/Dnac)) // FN
CORRECTED
cp_val40: TSFCinstalled=(WF/Fnet_installed)*36 // TSFC corrected
cp_val41: FIXED_DOH=1 // *****
cp_val42: P_propulsive=FN*V0 // Propulsive power
cp_val43: DoH_fixed=0.1 // Fixed degree of hybridisation
cp_val44: P_ex_fixed=DoH_fixed*P_propulsive/(1-DoH_fixed) // Power
extracted from fan

```

```

cp_val45: FanEff=0.585 // Fan efficiency
cp_val46: F_fan_fixed=FanEff*P_ex_fixed/V0*2 // Thrust produced by fan
cp_val47: Total_Thrust_fixed=F_fan_fixed+FN*2 // Total thrust produced
cp_val48: TSFC_fixed=(WF/Total_Thrust_fixed)*36/2 // TSFC in daN/kg/hr
cp_val49: Power_Outake_DOH_fixed=111.8+P_ex_fixed // Power offtake
cp_val50: PWX_fixed_Iter=PWX-Power_Outake_DOH_fixed // Total power
           offtake (Target = 0)
cp_val51: INSTALL_AND_FAN_EFFECTS=1 // *****
cp_val52: F_specific_installed=(Fnet_installed*100)/W2 // Specific
           Thrust in daNs/kg
cp_val53: TSFC_installed_FixedDOH=WF/(Fnet_installed+F_fan_fixed/2)*36
           // TSFC in daN/kg/hr
cp_val54: Specific_Thrust_FixedDOH=((Fnet_installed+F_fan_fixed/2)*100)/
           W2 // Specific Thrust in daNs/kg
cp_val55: ZP3q25 // HP comp ratio
cp_val56: ZP13q2 // Outer fan ratio

```

D.3 Design Point Cycle

Station	W kg/s	T K	P kPa	WRstd kg/s	FN	=	14.18
amb		218.81	23.842		TSFC	=	18.6696
2	95.394	246.88	35.990	248.588	WF	=	0.2647
13	84.794	283.41	55.781	152.757	s NOX	=	0.2068
21	10.599	283.41	55.781	19.095			
22	10.599	283.41	55.223	19.288	Core Eff	=	0.4631
24	10.599	283.42	55.228	19.286	Prop Eff	=	0.7628
25	10.599	283.42	54.124	19.679	BPR	=	8.0000
3	10.281	611.84	676.546	2.244	P2/P1	=	0.9900
31	9.708	611.84	676.546		P3/P2	=	18.80
4	9.973	1550.00	649.485	3.608	P5/P2	=	1.5822
41	10.272	1525.46	649.485	3.687	P16/P13	=	0.9800
43	10.272	1210.83	195.804		P16/P6	=	1.00000
44	10.546	1196.64	195.804		P16/P2	=	1.51887
45	10.846	1178.70	191.887	11.584	P6/P5	=	0.96000
49	10.846	906.04	56.943		P63/P6	=	1.00000
5	10.864	905.46	56.943	34.268	P163/P16	=	1.00000
6	10.864	905.46	54.665		XM63	=	0.48182
16	84.794	283.41	54.665		XM163	=	0.47050
64	95.659	359.46	54.070		XM64	=	0.50000
8	95.659	359.46	54.070	200.215	A64	=	1.11307
Bleed	0.000	611.84	676.545		WBld/W2	=	0.00000
-----					A8	=	0.84738
Efficiencies:	isent	polytr	RNI	P/P	CD8	=	0.98000
Outer LPC	0.9025	0.9083	0.426	1.550	XM8	=	1.00000
Inner LPC	0.9025	0.9083	0.426	1.550	PWX	=	485.7
kW							
IP Compressor	0.9500	0.9500	0.556	1.000	WBLD/W22	=	0.00000
HP Compressor	0.8937	0.9235	0.545	12.500	Wreci/W25	=	0.00000
Burner	0.9995			0.960	Loading	=	100.00
%							
HP Turbine	0.8578	0.8397	0.914	3.317	e444 th	=	0.84975

LP Turbine	0.9128	0.9000	0.363	3.370	WBLD/W25 =	0.00000
Mixer	0.6000				WCHN/W25 =	0.02821
-----					WCHR/W25 =	0.02590
HP Spool mech Eff	0.9900	Nom Spd	16082 rpm		WCLN/W25 =	0.02833
LP Spool mech Eff	0.9900	Nom Spd	4000 rpm		WCLR/W25 =	0.00167
P22/P21=0.9900	P25/P24=0.9800	P45/P44=0.9800			P6/P5 =	0.9600

hum [%]	war0	FHV	Fuel			
0.0	0.00000	43.153	Generic			

Composed Values:

- 1: COOLING_PARAMETERS_APPENDIX_B
= 1 *****
- 2: T_metal
= 1250 Metal Temperature
- 3: epsNGV
= 0.319774 Epsilon NGV
- 4: epsRotor
= 0.301501 Epsilon Rotor
- 5: CoolFrNGV
= 0.0282059 Cooling Fraction of NGV
- 6: CoolFrRotor
= 0.0258984 Cooling Fraction of Rotor
- 7: IterNGV
= 1.53974E-12 Iteration Variable for NGV 1 Cooling (Target = 0)
- 8: IterRot
= 4.04923E-13 Iteration Variable for Rotor 1 Cooling (Target = 0)
- 9: IterNGV2
= 1.53974E-12 Iteration Variable for NGV 2 Cooling (Target = 0)
- 10: IterRot2
= 4.04923E-13 Iteration Variable for Rotor 2 Cooling (Target = 0)
- 11: POLYTROPIC_EFFICIENCY_APPENDIX_B
= 1 *****
- 12: PolyEff_HPT_corrected
= 0.839694 HPT Efficiency reduced with cooling fraction correction
- 13: IterHPT_PolyEff
= 1 Iteration Variable for HPT Polytropic Efficiency (Target = 1)
- 14: n_stag_LPC
= 1 Number of Fan Stages
- 15: n_stag_IPC
= 3 Number of Booster Stages
- 16: n_stag_HPC
= 9 Number of HPC Stages
- 17: PiCstagLPC
= 1.54987 Stage Pressure Ratio of Fan
- 18: PiCstagIPC
= 1 Stage Pressure Ratio of Booster
- 19: PiCstagHPC
= 1.32397 Stage Pressure Ratio of HPC
- 20: IterFanRatio
= 1 Iteration Variable for Inner and Outer Fan Matching (Target = 1...)
- 21: PolyEffLPC
= 0.908338 Polytropic Efficiency of Fan
- 22: PolyEffIPC
= 0.95 Polytropic Efficiency of Booster

```

23: PolyEffHPC
   = 0.92347    Polytropic Efficiency of HPC
24: IterLPCin_PolyEff
   = 1          Iteration Variable for LPC (inner) Polytropic
               Efficiency (Target...)
25: IterLPCout_PolyEff
   = 1          Iteration Variable for LPC (outer) Polytropic
               Efficiency (Target...)
26: IterIPC_PolyEff
   = 1          Iteration Variable for IPC Polytropic Efficiency (
               Target = 1)
27: IterHPC_PolyEff
   = 1          Iteration Variable for HPC Polytropic Efficiency (
               Target = 1)
28: INSTALLATION_EFFECTS
   = 1          *****
29: kutta
   = 1          Kutta Condition (Target = 1)
30: NACELLE_DRAG
   = 1          *****
31: k_var
   = 0.04       Constant
32: NThrust
   = 14.1784    FN is given in kN
33: Dnac
   = 0.905535   Nacelle drag
34: Fnet_eff
   = 13.2729    FN effective
35: MTOW
   = 60160      MTOW
36: Area
   = 1.05893    Area that air passes through
37: d_fan
   = 1.21724    Diameter of fan
38: W_engine
   = 1378.47    Engine weight
39: Fnet_installed
   = 13.251     FN CORRECTED
40: TSFCinstalled
   = 0.719142   TSFC corrected
41: FIXED_DOH
   = 1          *****
42: P_propulsive
   = 3364.75    Propulsive power
43: DoH_fixed
   = 0.1        Fixed degree of hybridisation
44: P_ex_fixed
   = 373.861    Power extracted from fan
45: FanEff
   = 0.585      Fan efficiency
46: F_fan_fixed
   = 1.84319    Thrust produced by fan
47: Total_Thrust_fixed
   = 30.2       Total thrust produced
48: TSFC_fixed
   = 0.157771   TSFC in daN/kg/hr
49: Power_Outake_DOH_fixed
   = 485.661    Power offtake

```

```

50: PWX_fixed_Iter
   = 2.94196E-05   Total power offtake (Target = 0)
51: INSTALL_AND_FAN_EFFECTS
   = 1             *****
52: F_specific_installed
   = 13.8909       Specific Thrust in daNs/kg
53: TSFC_installed_FixedDOH
   = 0.672379     TSFC in daN/kg/hr
54: Specific_Thrust_FixedDOH
   = 14.857        Specific Thrust in daNs/kg
55: ZP3q25
   = 12.5          HP comp ratio
56: ZP13q2
   = 1.54987       Outer fan ratio

```

Iteration converged after 1 loops.

Iteration Variables:

1: Polytr.Inner LPC Efficiency (0.7...1)	= 0.908338
2: Polytr.Outer LPC Efficiency (0.7...1)	= 0.908338
3: Inner Fan Pressure Ratio (1...10)	= 1.54987
4: Polytr.IPC Efficiency (0.7...1)	= 0.95
5: Polytr.HPC Efficiency (0.7...1)	= 0.92347
6: HPT NGV 1 Cooling Air / W25 (0...0.3)	= 0.0282059
7: HPT Rotor 1 Cooling Air / W25 (0...0.3)	= 0.0258984
8: HPT NGV 2 Cooling Air / W25 (0...0.3)	= 0.0282059
9: HPT Rotor 2 Cooling Air / W25 (0...0.3)	= 0.0258984
10: Inlet Corr. Flow W2Rstd kg/s (0...1000)	= 248.588
11: Power Offtake kW (0...1000)	= 485.661
12: Polytr.HPT Efficiency (0.7...1)	= 0.839694
13: Outer Fan Pressure Ratio (1...10)	= 1.54987

Iteration Targets:

1: cp_val24	= 1
2: cp_val25	= 1
3: cp_val20	= 1
4: cp_val26	= 1
5: cp_val27	= 1
6: cp_val7	= 0
7: cp_val8	= 0
8: cp_val9	= 0
9: cp_val10	= 0
10: cp_val47	= 30.2
11: cp_val50	= 0
12: cp_val13	= 1
13: cp_val29	= 1

E GASTURB for Off-design

E.1 Off-Design Point Cycle

W	T	P	WRstd
---	---	---	-------

Station	kg/s	K	kPa	kg/s	FN	=	13.17
kN							
amb		218.81	23.842		TSFC	=	19.1505
g/(kN*s)							
2	90.508	246.88	35.990	235.857	WF	=	0.2523
kg/s							
13	79.195	286.35	57.585	138.913	s NOX	=	0.5276
21	11.314	286.35	57.585	19.845	P5/P2	=	1.4900
EPR							
22	11.314	286.35	57.009	20.045	Core Eff	=	0.4617
24	11.314	343.59	103.186	12.131	Prop Eff	=	0.7666
25	11.314	343.59	101.122	12.379	BPR	=	7.0000
3	11.087	742.21	1314.591	1.372	P2/P1	=	0.9900
31	10.259	742.21	1314.591		P3/P2	=	36.53
4	10.511	1575.00	1262.007	1.973	P5/P2	=	1.4900
41	10.946	1544.77	1262.007	2.035			
43	10.946	1131.79	249.885		P16/P6	=	1.09621
44	11.340	1119.21	249.885		P16/P2	=	1.56800
45	11.509	1112.02	244.888	9.355	P6/P5	=	0.96000
49	11.509	794.78	53.625		A8	=	0.16194
5	11.566	793.98	53.625	36.276	A18	=	0.60193
8	11.566	793.98	51.480	37.787	XM8	=	1.00000
18	79.195	286.35	56.433	141.748	XM18	=	1.00000
Bleed	0.000	742.21	1314.591		WBld/W2	=	0.00000
-----					CD8	=	0.98000
Efficiency		isent	polytr	RNI	CD18	=	0.97600
Outer LPC		0.9003	0.9067	0.426	PWX	=	893.4
kW							
Inner LPC		0.9003	0.9067	0.426	V18/V8,id=		0.62780
IP Compressor		0.9219	0.9281	0.567	WBLD/W22	=	0.00000
HP Compressor		0.8928	0.9227	0.810	Wreci/W25=		0.00000
Burner		0.9995			Loading	=	100.00
%							
HP Turbine		0.8552	0.8295	1.751	WCHN/W25	=	0.03840
LP Turbine		0.9161	0.9000	0.496	WCHR/W25	=	0.03483
-----					WCLN/W25	=	0.01500
HP Spool mech Eff	0.9900	Speed	18673	rpm	WCLRW25	=	0.00500
LP Spool mech Eff	0.9900	Speed	4000	rpm	WBLD/W25	=	0.00000
-----					P6/P5	=	0.96000
P22/P21=0.9900	P25/P24=0.9800	P45/P44=0.9800			P16/P13	=	0.9800

hum [%]	war0	FHV	Fuel				
0.0	0.00000	43.153	Generic				
All iteration variables estimated correctly - no iteration needed.							
Spool Speeds:							
Absolute [RPM]		LP Spool	IP Spool	HP Spool			
Relative		4000.0	4000.0	18672.6			
		1.0000	1.0000	1.0000			
		LPC	IPC	HPC			
Surge Margin [%]		45.477	56.467	24.104			
Handling Bleed WB,hd/W22			0.0000				
Map Coordinates:							
LPT		LPC	IPC	HPC	HPT		
Map Speed		1.0000	1.0000	1.0000	1.0000		
1.0000							

Map Coordinate Beta 0.5000	0.5000	0.4000	0.5000	0.5000	
Reynolds Corrections: LPT	LPC	IPC	HPC	HPT	
Efficiency 0.9848	1.0000	0.9877	0.9954	1.0000	
Flow 0.9924	1.0000	0.9938	0.9977	1.0000	
Modifiers: LPT	Bypass-LPC-Core		IPC	HPC	HPT
Delta Efficiency [%] 0.000	0.000	0.000	0.000	0.000	0.000
Delta Flow Capacity [%] 0.000		0.000	0.000	0.000	0.000
Delta Core Nozz Area [%]	0.000				
Delta Byp Nozz Area [%]	0.000				
Delta Core Inl Duct P/P [%]	0.000				
Delta Comp Interd P/P [%]	0.000				
Delta Burner P/P [%]	0.000				
Delta Turb Interd P/P [%]	0.000				
Delta Turbine Exit P/P [%]	0.000				
Delta Bypass P/P [%]	0.000				